Paleomagnetism and U–Pb geochronology of easterly trending dykes in the Dharwar craton, India: feldspar clouding, radiating dyke swarms and the position of India at 2.37 Ga

H.C. Halls [a,*], A. Kumar [b], R. Srinivasan [c], M.A. Hamilton [d]

[a] *Department of Chemical and Physical Sciences, University of Toronto at Mississauga, Mississauga, ON L5L 1C6, Canada*
[b] *National Geophysical Research Institute, Uppal Road, Hyderabad 500 007, India*
[c] *Australian Indian Resources Pty. Ltd, Bangalore, India*
[d] *Jack Satterly Geochronology Laboratory, Department of Geology, University of Toronto, Toronto, ON M5S 3B1, Canada*

Abstract

A U–Pb baddeleyite age of 2367 ± 1 Ma from a diabase dyke together with previously published age data, suggests that a major early Proterozoic dyke swarm cuts across the structural grain of the Archean Dharwar craton in India. Paleomagnetic data suggest the swarm is at least 300 km wide and 300 km long and has a fan angle of at least 30° with convergence to the west. It was originally emplaced at high latitudes, and together with the Widgiemooltha dykes of the Yilgarn block of Australia, may have been a segment of a larger radiating swarm related to a long-lived plume event that was active for about 50 My from 2418 to 2367 Ma. A regional change in the intensity of brown feldspar clouding in the dykes suggests that the Dharwar craton was tilted northwards, in harmony with previous observations on the structure and metamorphism of the Archean rocks. Towards the south the brown feldspar clouding becomes more intense and locally assumes a blacker, more "sooty" appearance. The black clouding, whose precise origins remain unknown, is accompanied by a remagnetization and appears to coincide closely with a region of carbonatite magmatism at ∼800 Ma, and with a shear zone and change in structural trend related to Pan-African deformation at ∼550 Ma. Paleomagnetic studies suggest that (i) the high coercivity part of the remanent magnetization is carried by magnetite exsolved within either brown or black clouded feldspars and (ii) as a more general observation, diabase with brown clouded feldspar can carry a primary magnetization but not if the clouding is black.

© 2007 Elsevier B.V. All rights reserved.

Keywords: Dyke swarms; Dharwar craton; Dykes; India; Paleomagnetism; U–Pb geochronology; Cloudy feldspar

1. Introduction

The first map exclusively devoted to dyke distributions within the eastern half of the Archean Dharwar craton of India (Halls, 1982) showed several sets of dykes traced from satellite Landsat imagery. The most prominent set, in terms of numbers and length of individual dykes, was approximately normal to the trend of the Archean granite-greenstone terranes. Since the Archean structural grain has a curvature that opens westward (Fig. 1), the dyke distribution is fan shaped with a convergence towards the west. It was originally speculated that because the earliest dyke swarms in Archean cratons are generally orthogonal to Archean structural grain (Halls, 1978), the Indian dykes were about 2.4 Ga old (Halls, 1982, Fig. 1). However subsequently the full

* Corresponding author. Tel.: +1 905 828 5363;
fax: +1 905 828 3717.
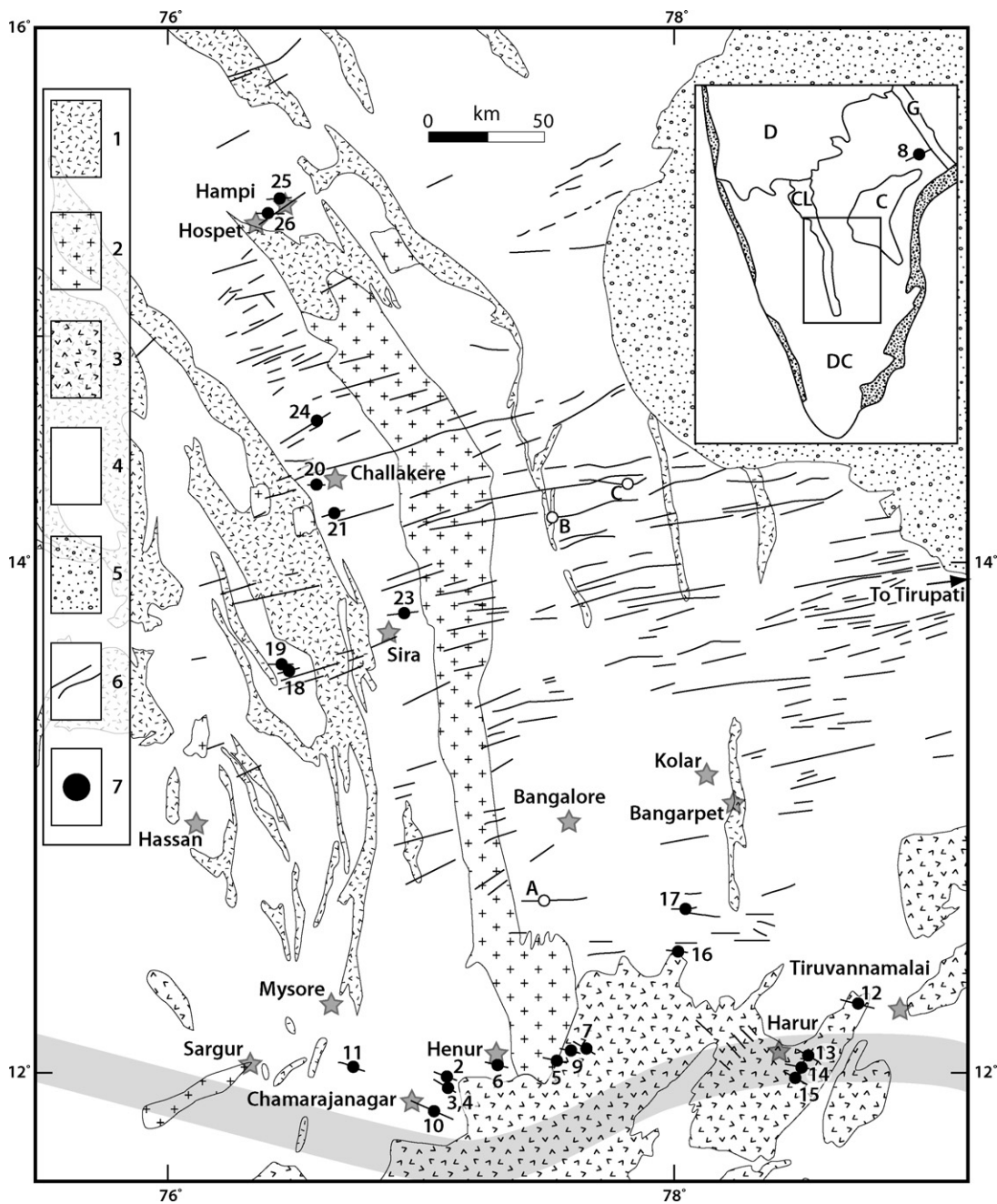*E-mail address:* hhalls@utm.utoronto.ca (H.C. Halls).

Fig. 1. Geological sketch map of the central Indian Peninsula showing the main rock types of the Archean Dharwar craton, dykes that have general E-W trends and their paleomagnetic sampling sites. Legend: Archean: 1—supracrustal rocks; 2—Closepet and related granites; 3—charnockites and other high grade rocks; 4—gneisses and granite gneisses. Paleoproterozoic: 5—Sedimentary rocks of the Cuddapah basin; 6—basaltic dykes. 7—Paleomagnetic sites. Inset of Peninsula India: DC—Dharwar Craton; CL—Closepet granite; G—Godavari rift; C—Cuddapah basin; D—Deccan plateau basalts (Cretaceous). The locations A, B and C refer to key dykes that are discussed in the text. A major Pan African (∼550 Ma) shear zone is shown schematically in grey shading (after Drury and Holt, 1980).

extent of the large radiating 2.45 Ga Matachewan swarm in Canada has been defined (Halls and Bates, 1990), cutting an Archean granite-greenstone terrain that maintains a uniform structural trend, so that the orthogonal rela-

tion as a general rule is now less apparent and instead greater emphasis has been placed on fan-shaped or radiating swarms as defining the loci of feeder plumes (e.g. Ernst and Buchan, 2001).

In this paper we present new paleomagnetic and U–Pb age data that provide a key early Proterozoic paleomagnetic pole for the Indian subcontinent, and which bear upon the reality or otherwise of the postulated fan-shaped swarm from the Dharwar craton.

2. General geology

The Dharwar craton of India is formed of four major units: the Peninsular gneisses forming a typical Archean TTG gneiss terrain, greenstone belts, metasedimentary rocks, and late potassic granites, such as the Closepet granite (Fig. 1), dated at ∼2.5 Ga (Friend and Nutman, 1991), that form the final Archean magmatic event. The craton can broadly be divided into older western (Western Dharwar Craton: 3.3–2.7 Ga) and younger eastern (Eastern Dharwar craton: 3.0–2.5 Ga) blocks (Swami Nath and Ramakrishnan, 1981; Naqvi and Rogers, 1987; Chadwick et al., 2000). The regional metamorphic grade changes gradually southwards across the craton as a whole from greenschist facies in the north to granulite facies in charnockitic terrains in the south (Fig. 1). Rb–Sr whole rocks ages from granites and gneisses in the eastern Dharwar craton range from about 2545 to 2128 Ma (Table 1 of Pandey et al., 1997), suggesting that Archean ages have been variably reset by a regional event at ∼2.1 Ga. Paleoproterozoic sedimentary rocks overlie the Archean basement and include the Cuddapah basin which is crescent-shaped with gentle easterly dips in the map area (Fig. 1). Within the Cuddapah basin, volcanics occur about 2 km above the base of the sequence and associated sills give a Rb–Sr whole rock–mineral

Table 1
Compilation of previous published and unpublished paleomagnetic data from easterly trending dykes

SITE	LAT	LONG	T	W	N	D	I	P_{lat}	P_{lon}	α_{95}	k	Reference
12	**12.66**	**77.50**	**270**	**15**	**6**	**135.1**	**−84.7**	**20.0**	**69.6**	**6.4**	**110**	**1**
15	**12.65**	**77.42**	**295**	**15**	**6**	**72.6**	**−78.1**	**5.1**	**55.6**	**7.4**	**84**	**1**
16	**12.66**	**77.42**	**265**	**15**	**5**	**60.3**	**−81.2**	**3.8**	**62.5**	**7.4**	**109**	**1**
C-VI	12.11	79.13	300		5	116	−75			6	127	2
C-VII	12.16	79.03	300		7	112	−77			6	87	2
C-T7	12.05	79.09	300		7	92.1	−70.7			7.3	69	3
C	**12.11**	**79.08**	**300**		**3[a]**	**105.2**	**−74.5**	**17.9**	**49.6**	**7.4**	**280**	**2, 3**
E	**12.11**	**79.07**	**030**		**6**	**115**	**−75**	**22.3**	**51.5**	**7**	**75**	**2**
F	**12.21**	**79.08**	**300**		**4**	**125**	**−75**	**26.8**	**53.4**	**9**	**58**	**2**
T3	**12.09**	**78.92**	**300**		**7**	**129.7**	**−73.5**	**29.9**	**52.0**	**2.8**	**481**	**3**
D7	**12.08**	**77.89**	**295**		**6**	**105.8**	**−75.5**	**18.0**	**50.2**	**5.2**	**168**	**3**
T4	**12.06**	**79.01**	**030**		**7**	**114.4**	**−67.9**	**24.6**	**39.8**	**9.6**	**92**	**3**
i = A + B	**14.19**	**77.64**	**255**		**5**	**56.5**	**−69.5**	**−7.1**	**47.4**	**7**	**53**	**4**
ii = C	14.20	77.81	255		4	88	−73			3	185	4
ii = D	14.20	77.80	255		4	71	−74			2	547	4
ii = J	14.14	77.66	240		5	59	−70			10	48	4
ii	**14.18**	**77.76**	**250**		**3[a]**	**71.9**	**−72.7**	**2.8**	**47.5**	**7.5**	**271**	**4**
ii = Z[b]	14.20	77.81			3	56	−68			11	55	4
1	**12.90**	**78.20**	**?**		**7**	**170**	**−80**	**32.0**	**74.3**	**5.0**	**113**	**5**
2	**12.90**	**78.20**	**?**		**6**	**88**	**−81**	**11.7**	**60.3**	**6.3**	**82**	**5**
3	**12.90**	**78.20**	**?**		**9**	**127**	**−77**	**26.7**	**56.2**	**4.2**	**124**	**5**
BANG	**12.90**	**78.20**	**?**		**3[a]**	**129.4**	**−80.9**	**23.7**	**63.3**	**10.8**	**131**	**5**
10	**12.73**	**77.52**	**280**		**4**	**141.0**	**−75.0**	**33.5**	**56.6**	**10.0**	**50**	**6**
Hol [1]	**12.79**	**76.23**	**310**	**50**	**4**	**62.2**	**−78.4**	**1.8**	**56.6**	**3.0**	**916**	**7**
Hol [2]	**12.79**	**76.23**	**065**	**8**	**4**	**54.7**	**−79.2**	**0.3**	**59.3**	**6.2**	**218**	**7**

Notes: Results satisfy the following acceptance criteria: number of samples $N \geq 4$, and $\alpha_{95} \leq 15°$. Results in bold type are those for individual dykes. Where more than one site occurs in the same dyke, the SITE results are shown in plain type. Column headings: SITE refers to the original site names referred to in the publications; LAT, LONG: site lat (°N) and longitude (°E); T—dyke trend (°); W—dyke width where specified (m); N—number of independently oriented samples used to calculate magnetization direction given by D, declination and I, inclination (°); P_{lat}, P_{lon}—latitude (°N) and longitude (°E) of virtual paleomagnetic pole position; α_{95} is the radius (°) of the 95% circle of confidence about the mean magnetization direction; k is Fisher's precision parameter and Reference is the number of the reference: 1: Dawson and Hargraves (1994); 2: Venkatesh et al. (1987); 3: Radhakrishna and Joseph (1996); 4: Kumar and Bhalla (1983); 5: Bhalla et al. (1980); 6: Hasnain and Qureshy (1971); 7: Sites from canal cutting at Holenarsipur (A. Kumar, unpublished data, 1985). Mean direction and paleomagnetic pole for the accepted data are given in Table 5.
[a] Number of sites.
[b] Older diabase baked by dyke ii.

isochron age of 1817 ± 24 Ma (Bhaskar Rao et al., 1995) and Ar–Ar laser fusion ages on phlogopite that average 1899 ± 20 Ma (Anand et al., 2003). The age of the oldest clastic sediments that rest directly on the basement is therefore greater than ~ 1.9 Ga. The lack of deformation in the western Cuddapah basin shows that the curvature in the units of the Dharwar craton is at least older than ~ 2 Ga and was probably established by the end of the Archean.

The southern boundary of the Dharwar craton is marked by a major shear zone in amphibolite facies, that appears to have been active during Pan African orogenic activity at ~ 550 Ma and which separates the craton from high grade, charnockitic Pan-African terranes to the south (Meissner et al., 2002; Santosh et al., 2003). Across this shear zone which occurs close to many of our sampling sites (Fig. 1), the dominant NNW-trending structural grain of the Dharwar craton changes to one with an E to NE trend. At the eastern end of this shear zone in the vicinity of Harur a number of carbonatite and associated syenite intrusions occur. The age of this igneous activity is close to 800 Ma (Kumar et al., 1998, mica and whole rock Rb–Sr isochrons of 770 Ma; Schleicher et al., 1998, whole rock Pb–Pb age of 801 ± 11 Ma).

3. Proterozoic dyke swarms of the Eastern Dharwar craton

A basic problem that has hindered until recently the emergence of a coherent picture of dyke swarm emplacement across the Dharwar craton is that the majority of radiometric ages have been obtained by the K–Ar method or its variant, Ar–Ar step heating, and are therefore susceptible to error either by inherited argon or by argon loss. From cross-cutting field relations, together with whole rock K–Ar and paleomagnetic data, at least four ages of dykes swarms have been proposed in different areas of the craton (Anjannappa, 1975; Gokhale and Waghamare, 1989; Radhakrishna and Joseph, 1996; Poornachandra Rao, 2005). On a more regional scale, from aerial photo, aeromagnetic and field studies, as many as five different episodes of dyke intrusion have been proposed around the Cuddapah basin (Murty et al., 1987). Most of the dykes are quartz tholeiites and have trends that are typically E–W, NE and N, but more alkaline dykes, sometimes with olivine, have N and NW trends (Murty et al., 1987, their Table 1).

Published paleomagnetic data from the Dharwar craton up to 1980 was reviewed by Hargraves and Bhalla (1983) who demonstrated that the various studies of dyke swarms gave widely scattered and sometimes conflicting

data. The relatively low reliability of both the paleomagnetic and K–Ar radiometric data as judged by their associated error estimates may explain the lack of agreement between data from different parts of the craton, with the result that no convincing pattern of dyke swarm intrusion, either spatially or temporally, has emerged. The range in K–Ar or Ar–Ar ages on dykes has been taken to mean that the craton has been subjected to many dyking episodes between 650 and 2400 Ma (e.g. Radhakrishna and Joseph, 1996; Poornachandra Rao, 2005). However, a key observation from both Landsat images and field studies is that of the hundreds of dykes having several trends in the vicinity of the Cuddapah basin (Murty et al., 1987), only one has been observed to cut the basal sedimentary units (see Anand et al., 2003), which suggests that the vast majority of the dykes intruded before ~ 1.9 Ga.

Radiometric dating using the Sm–Nd, Rb–Sr and U–Pb methods is beginning to confirm that the dykes *are* mainly Paleoproterozoic in age and comprise two major magmatic episodes centred at ~ 2.1 and ~ 2.4 Ga. An E–W trending dyke at location A in Fig. 1 yielded a Rb–Sr age of 2370 ± 230 Ma (Ikramuddin and Stueber, 1976) and another dyke of the same trend at location B in Fig. 1 has given a Sm–Nd age of 2454 ± 100 Ma from a 7-point whole rock–mineral isochron (Zachariah et al., 1995). Sm–Nd data from three NW-trending mafic dykes in a region centred on $16.7°N$ $77.7°E$, NW of the Cuddapah basin in Fig. 1, yield an isochron age of 2173 ± 64 Ma (Pandey et al., 1997). More recently, the Paleoproterozoic ages have been confirmed by U–Pb age data on baddeleyite and zircon from 11 dykes across the Dharwar craton showing that the igneous activity is bracketed between 2.4 and 2.0 Ga, and includes a U–Pb baddeleyite age of 2365.5 ± 1.1 Ma from the dyke at location A (French et al., 2004). The disturbed isotopic systems in Archean rocks summarised in Table 1 of Pandey et al. (1997) may in part reflect these Paleoproterozoic magmatic events.

Paleomagnetic studies on dykes from the Dharwar craton have proven challenging because surface outcrops are frequently lightning-struck, and quarries and road cuts containing fresh exposures are relatively rare. It has been demonstrated (e.g. Halls, 1991) that the most stable, highest coercivity and unblocking temperature remanences in Canadian Paleoproterozoic dykes come from chilled margins, where magnetite grain sizes are small. In India the preservation of fresh chilled margins is relatively rare, so that many paleomagnetic studies, particularly those prior to ~ 1980 have not stressed chilled margins in sampling strategies, with the result that interior samples have yielded generally low coer-

civity remanences. These magnetizations show a large within-site directional dispersion because of the difficulty in separating them from more dominant lightning and recent weathering components.

A key paleomagnetic study was that by Dawson and Hargraves (1994) who obtained a stable characteristic remanence with a steep negative inclination from three E–W trending dykes at location A (including the one dated by the U–Pb dated method), southwest of the Cuddapah basin. In the same area a steep down direction characterised N–S trending alkaline dykes one of which yielded a Rb–Sr age of 810 ± 25 Ma (Ikramuddin and Stueber, 1976). A second key paper was that by Kumar and Bhalla (1983) who reported an easterly dyke (location C in Fig. 1), also with a steep negative inclination ($D = 70°$ $I = -73°$), that yielded a positive baked contact test where it was observed to cut another dyke with NE trend from which three sites remote from the intersection gave a consistent magnetization direction that averaged $D = 64$, $I = -7°$. This result suggests that the steep negative direction as found in easterly trending dykes is a primary one. No paleomagnetic work has been done on the dyke at location B in Fig. 1. A summary of the most reliable published paleomagnetic results that show a steep negative inclination indicates that nearly all of them are from WNW to ENE trending dykes (Table 1 and Fig. 2). A notable exception occurs in the granulite terranes of the southern Dharwar where NE trending dykes also show the steep negative component (Radhakrishna and Joseph, 1996).

In a seminal paper Pichamuthu (1959) showed that the mafic dykes of the Dharwar craton show increased cloudiness of their groundmass feldspars towards the south. A similar observation occurs in the 2445 Ma Matachewan dyke swarm of Canada where it was shown that the clouding is the result of the exsolution of magnetite and other minerals, possibly including amphibole, from the feldspar lattice as a result of slow cooling at large crustal depths (Halls and Zhang, 1995, 2003). The intensity of the clouding was shown to increase with the depth of exhumation in the Matachewan swarm, so that it gives a crude measure of the crustal depth at which the exposed part of the dyke originally resided. In the Dharwar craton, granite and volcano-sedimentary belts at greenschist facies metamorphism pass southwards to higher grade charnockitic terranes in granulite facies. This, together with the increased clouding of the groundmass feldspars and the analogous properties of Matachewan dykes (Halls and Zhang, 1995), suggests that the craton has been tilted northwards following the emplacement of the dykes. This conclusion is in harmony with previous observations of NNW-plunging folds in

the Archean (Pichamuthu, 1953) and petrological studies of the Closepet granite that show a northward decrease in crustal depth from about 26 to 14 km in 300 km (Moyen et al., 2003).

In Canada the Matachewan dykes that exhibit feldspar clouding, have been uplifted at approximately 2.0 Ga, some 20 km along a major crustal uplift known as the Kapuskasing Zone, yet still retain a paleomagnetic direction that is similar to dykes from shallower crustal levels outside the uplifted area. It was shown that the clouding causes a stable, high coercivity remanence that resides in the fine-grained magnetite exsolved in the feldspars, and that this remanence dated from the general time of Matachewan igneous activity rather than being a product of a later geological event (Halls and Zhang, 2003).

4. Field and experimental methods

4.1. Geochemistry and petrography

To help identify dykes that are geochemically distinct from others and which may therefore belong to different magmatic episodes, 20 samples of chilled margins, representing 12 different dykes, were analysed for major, minor and trace elements. Lower detection limits are ± 0.01 % for major elements and approximately 2 ppm for Rb, Sr, and Y, 3 ppm for Zr, 5 ppm for Cr and 20 ppm for Ba. Petrographic thin sections were obtained for all dyke interiors, with particular attention paid to clouding intensity of the feldspars as originally reported by Pichamuthu (1959). Polished thin sections were also obtained for reflected light examination and for use on the scanning electron microscope in the Geology Department, University of Toronto, in order to study the nature of the feldspar clouding.

4.2. U–Pb geochronology

All U–Pb analytical work was carried out in the Jack Satterly Geochronology Laboratory (JSGL) at the University of Toronto. Samples for geochronology were collected from quarries in the central, coarse-grained portion of a 20–30 m thick diabase dyke, striking 290°, at paleomagnetic site 2, near Yeragumballi (WSW of Henur, Fig. 1). A small quantity (approximately 0.25 kg) of fresh drill core material was crushed and finely ground using standard jaw crusher and disc mill techniques, and then decanted in water of its suspended fines. The residue was treated with conventional heavy liquid methods and Frantz^{TM} isodynamic magnetic separation techniques in order to isolate the least magnetic grains within the dense mineral fractions. Roughly 20 grains
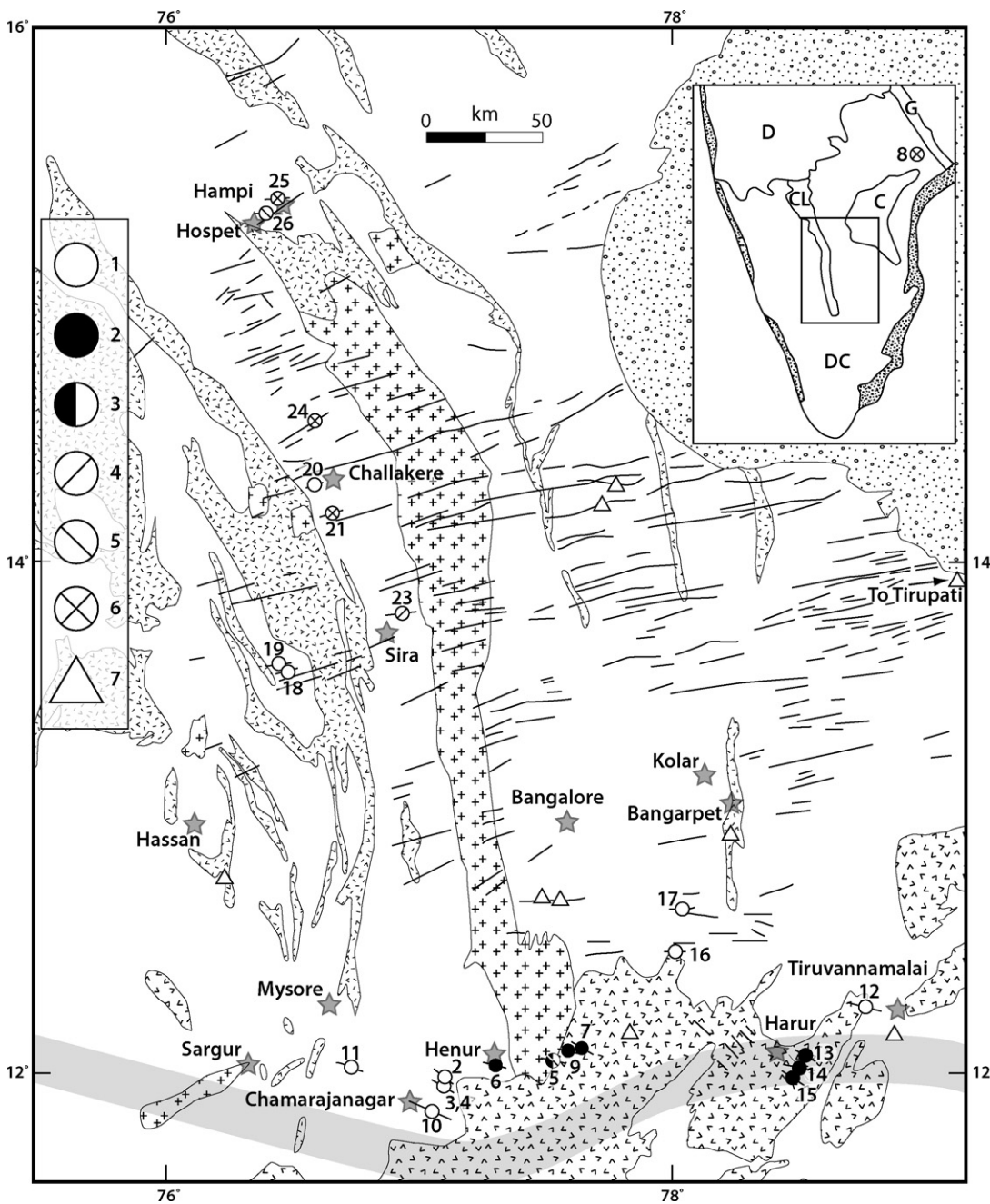
Fig. 2. Site locations from the present study are coded according to their characteristic paleomagnetic components: 1—A; 2—B; 3—A and B occurring together; 4—component antipodal to A; 5—component C; 6—unstable, no coherent remanence; 7—approximate locations where previous paleomagnetic studies on dykes have revealed component A according to Table 1; each symbol may include more than one study if they are in the same area. Note that sites carrying A occur throughout the map, but dykes containing B are confined to the extreme southern part of the map and either lie within or up to several tens of kilometres north of the major Pan African shear zone, shown in grey shading.

of baddeleyite were recovered from the entire separation procedure – all being thin, bladed morphologies less than 100 μm in longest dimension (most were <50 μm). Highest quality grains of baddeleyite were handpicked under ethanol using a binocular microscope and selected

for isotopic analysis. Prior to dissolution, weights of selected fractions were estimated by use of a scaled digital photographic measurement of the length and breadth of each component grain, and an estimate of the maximum thickness, together with the known density.

Isotope dilution U–Pb analytical work broadly followed the sample preparation and laboratory methods described by Hamilton et al. (2002). Following dissolution in concentrated HF mixed with ^{205}Pb–^{235}U spike and conversion to chloride, the samples were loaded, without column chemistry, directly onto Re filaments with Si-gel and phosphoric acid. Isotope ratios were measured on a VG354 mass spectrometer using a Daly detector equipped with digital ion counting. System deadtime corrections during this period were 20 ns for Pb and U. Detector characteristics were monitored during the analytical period using the SRM-982 Pb and CBNM 072/6 U standards. Corrections were 0.07%/amu for Daly mass discrimination and 0.10%/amu for thermal mass discrimination. JSGL procedural blanks are normally at the 0.5 and 0.1 pg level for Pb and U, respectively. The measured total common Pb in the samples was low and was assigned the common Pb composition of the lab blank. Comprehensive error estimation was made by propagating all known sources of analytical error and uncertainties in the composition of the blank. Decay constants used are those of Jaffey et al. (1971). Age regression and errors were calculated using the algorithms of Ludwig (2003). Concordia ellipse errors and calculated age are shown at the 95% confidence level of uncertainty. U–Pb Concordia diagram was generated using the Microsoft Excel Add-in IsoPlot/Ex v.3.0 (Ludwig, 2003).

4.3. Paleomagnetism

A total of 24 paleomagnetic sites were obtained from ENE – to ESE – trending dykes (Fig. 1), comprising on average about six block samples oriented by both sun and magnetic compass. Many sites lacked chilled margins, a few were in quarries but most were from natural outcrops. After the blocks were cored, the cores were cut into cylindrical specimens 2.45 cm in length and in diameter. At least one specimen per sample was subject to detailed stepwise alternating field (AF) demagnetization, using a Schonstedt TD-1 instrument, to a maximum field of 100 mT, in order to separate components by their coercivity. Thermal demagnetization using a Schonstedt TSD-1 was also carried out on selected specimens and sometimes on those that had previously been AF demagnetized. After each incremental demagnetization step, the natural remanent magnetization (NRM) was measured at the Erindale paleomagnetic laboratory on a modified DIGICO magnetometer with reproducibility down to 10^{-3} Am^{-1}. This instrument is equipped with a software routine designed to average out variations in magnetization directions that are a function of the last demagnetization axis in single axis demagnetizers and which become more apparent once the NRM intensity falls below about 20% of its initial value. This averaging routine was particularly important in the Indian samples because the characteristic component was often only isolated below 5% of the NRM intensity. The directional data were then analysed using Principal Component Analysis (Kirschvink, 1980) in combination with stereoplots and vector diagrams, following normal paleomagnetic procedures. Acceptance criteria for linear segments on vector diagrams were: number of consecutive demagnetization points $\geq$3 and the maximum angle of deviation (Kirschvink, 1980) $\leq$10°. The variation of susceptibility as a function of temperature to 700 °C, using a Sapphire Instruments SI3 meter, was also obtained on selected samples in order to identify remanence carriers.

5. Results

5.1. Petrography

5.1.1. Primary mineralogy and texture

Representative photomicrographs of all dykes are characterised by approximately equal proportions of clinopyroxene and plagioclase constituting about 90% of the rock (Fig. 3). The clinopyroxene is subhedral, occasionally anhedral, and the overall texture is equigranular, rarely sub-ophitic. Accessory minerals form the remaining 10% and approximately in order of abundance are: (1) a strongly pleochroic (yellow green to blue green) amphibole which rims the clinopyroxene and also occurs as isolated grains; (2) myrmekite, often with larger areas of quartz; (3) biotite and magnetite, often intergrown; (4) orthopyroxene in corroded grains lying with clinopyroxene and (5) apatite needles, abundant in areas of myrmekite. In the lower metamorphic grade areas of the Dharwar craton, chlorite and uralite become more conspicuous. Baddeleyite and/or zircon may be responsible for pleochroic haloes seen in amphibole, biotite and chlorite grains but due to the paucity of these minerals in most of the dykes, only sites 2, 10 and 25 were identified as possible candidates for U–Pb dating. Olivine, titanite and epidote were not positively identified in any of the thin sections. All the dykes are extremely similar in their primary mineralogy and texture and differ only in degree of alteration.

5.1.2. Alteration

In the more northern sites, pyroxene is more altered to a fibrous amphibole (probably uralite) and dirty aggregates, and plagioclase is more saussuritised. However in
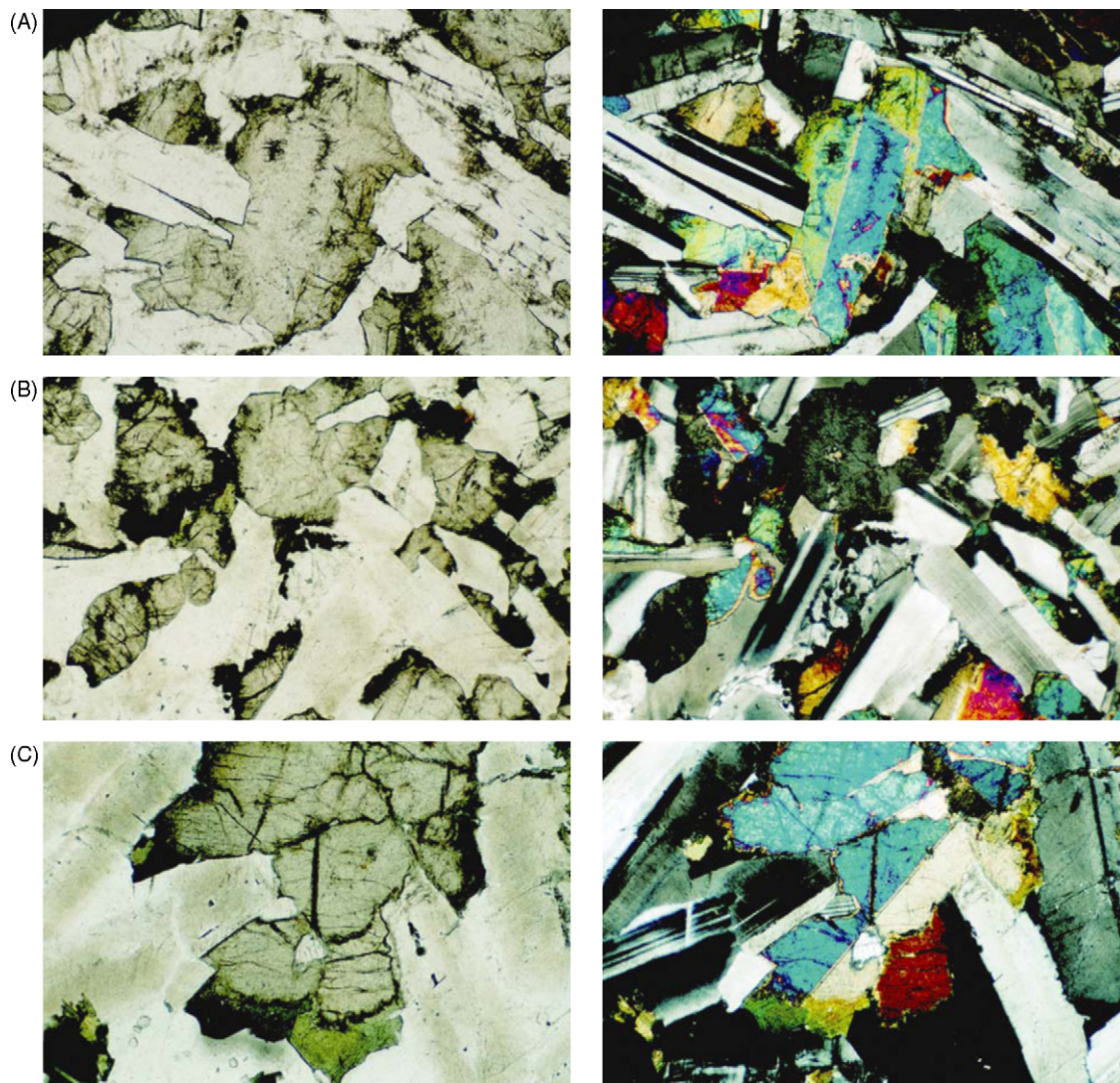
Fig. 3. Photomicrographs from three dyke interiors showing increased feldspar clouding towards the south. Plane light photos (on left) with companion ones under crossed nicols on right (photo width 2.5 mm). The feldspar clouding is shown in the plane light photos which are arranged, top down from north to south. The photos on the right show clearly defined feldspar twinning and no saussuritization, demonstrating that the clouding is not a low temperature hydrous alteration. Other minerals are clinopyroxene (grey under plane light, with second order birefringence colours under crossed nicols), an amphibole (green under plane light) often rimming the pyroxene, and magnetite (black in both photos). The second order interference for pyroxene demonstrates that the sections are of comparable thickness and that variations in slide thickness are not responsible for the variation in feldspar clouding. Clear white areas with hexagonal or needle shaped apatite inclusions are quartz/feldspar intergrowths. A: Site 19, B: Site 16, C: Site 10.

either mineral the alteration seldom exceeds about 40%. Most dykes, particularly from the higher-grade southern areas, are fresh; both clinopyroxene and plagioclase are generally 90% unaltered. Here also the plagioclase has a noticeable brown tea-coloured clouding which becomes progressively less intense towards the north (Fig. 3). Where clouded, the plagioclase is locally suffused with tiny inclusions. In some sites, the clouding has a blacker, more "sooty" appearance compared to the brown clouding (Fig. 4) and where well developed, the plagioclase also becomes crowded with more inclusions including needle-shaped ones that are often aligned along different crystallographic directions (Fig. 4, photo H). The two types of clouding were originally reported by Pichamuthu (1951) who also briefly described the needle-shaped inclusions. Those sites (5–7, 9, 13–15) displaying the sooty behaviour occur in the extreme southern areas and to the east of a group of dykes (sites
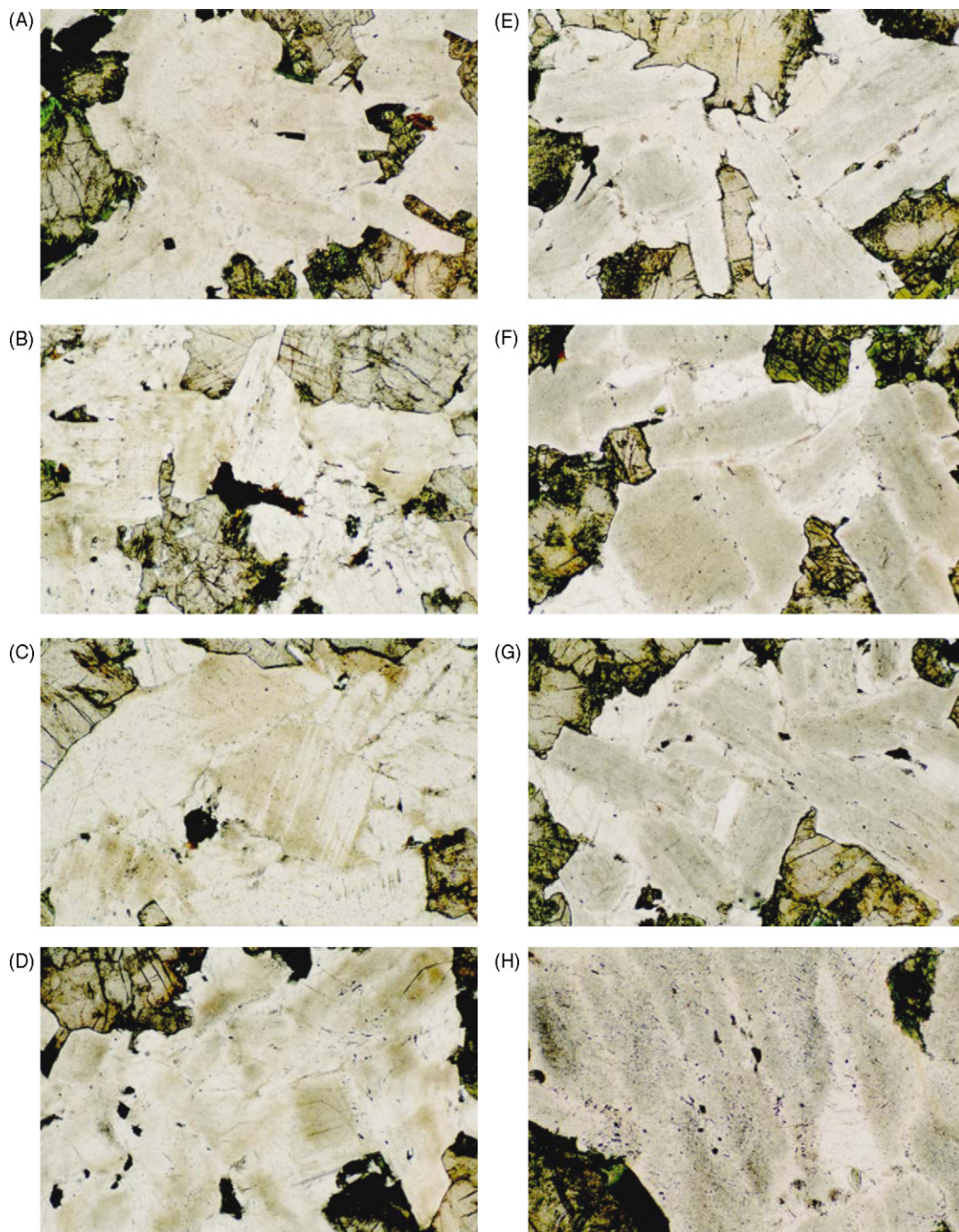
Fig. 4. Plane light photomicrographs showing dykes with brown "tea" clouding of feldspar on the left, compared with dykes which show a blacker, "sooty" clouding on the right. The pictures are arranged from top to bottom in order of increasing clouding intensity. Photo A—site 2; B—site 11, C—site 4, D—site 3 [note a more intense tea clouding with some sooty development], E—site 5; F—site 7; G—site 15 and H—site 6 (note the appearance of needle-shaped inclusion aligned along crystallographic planes when sooty development becomes more intense). All photo widths are 2.5 mm except for photos C and H which are 1.2 mm.
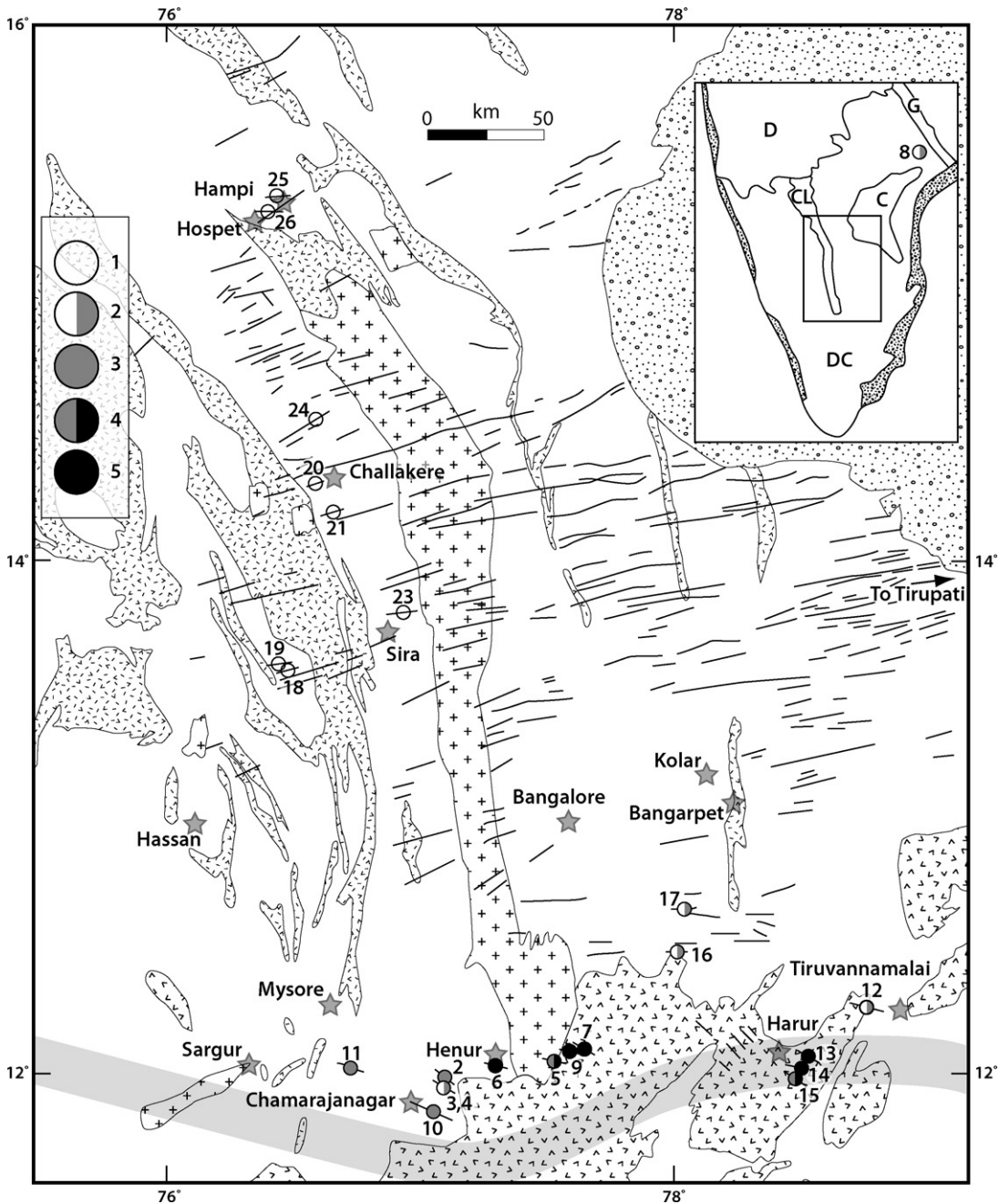
Fig. 5. Site locations coded according to the degree and type of feldspar clouding: 1—clear feldspar; 2—low to intermediate brown clouding; 3—intermediate to heavy brown clouding; 4—samples as in 3 but showing partial replacement of brown clouding by black; 5—heavy to intermediate black or sooty clouding. Note strong correlation between dykes that carry the B component in Fig. 2 and those that carry the black sooty clouding. Also note that these dykes either lie within or immediately north of the shear zone shown in grey shading, whereas all A sites lie north of the zone. The irregular and sharp line between dykes with brown and black clouding may be because of a shallow dip of the shear zone, other related but unmapped faults, or because a wider region of associated alteration flanks the fault zone. In the Harur area fenitization associated with ∼800 Ma carbonatites may also be responsible for B.

2–4, 10, 11) all of which show the brown tea colour (Fig. 5). At all sites deformation in the form of shearing and slickenlines along margins and joints is absent, except at sites 13 and 15 where the dykes also show bleaching along joints and epidote veining. In polished thin sections, tiny magnetite inclusions were visible in both brown and black-clouded feldspars but were more numerous in the latter.

5.2. Geochronology

Results of U–Pb isotopic analyses for four fractions of baddeleyite from the diabase dyke at site 2 are presented in Table 2. Fractions consisted of only 2 or 3 crystals of baddeleyite each. These grains show moderate levels of uranium (120–386 ppm) and consistently low Th/U ratios (0.01). The data for three fractions are mostly clustered, approximately 1.5% discordant, while a fourth shows only minor Pb-loss (0.6% discordant), and all fractions show a very restricted total range of $^{207}Pb/^{206}Pb$ ages (2366.1–2367.4 Ma). The consistent dispersion of the data produces a well-defined co-linear array (Fig. 6). When the data are fitted to a line constrained to have a zero-aged (geologically recent) lower Concordia intercept, the regression yields an upper intercept age of 2366.7 ± 1.0 Ma (2σ, MSWD = 0.38, 76% probability of fit). This result is interpreted to represent a highly reliable and precise age of emplacement and crystallization of the approximately WNW-trending (290°) dyke at site 2.
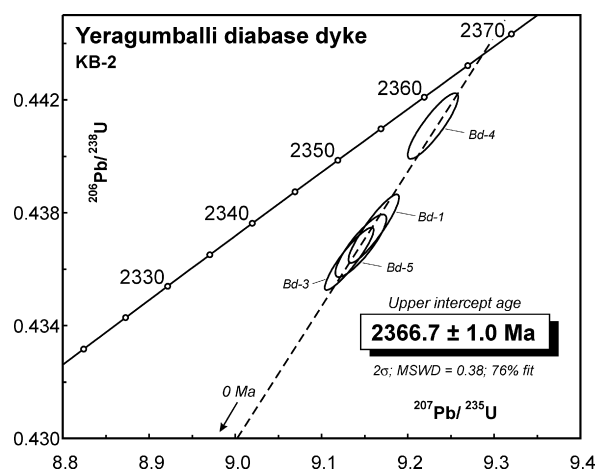

Fig. 6. Concordia diagram showing U–Pb dating results for four fractions of baddeleyite from the Yeragumballi (Yelandur) diabase dyke, site 2. Regression of all data, assuming recent Pb-loss, yields a Concordia upper intercept of 2366.7 ± 1.0 Ma, taken to represent the emplacement age of the dyke.

Table 2
U–Pb analytical results for baddeleyite from the Yeragumballi dyke, paleomagnetic site 2, near Henur

Sample fraction	Analysis no.	Description	Weight (mg)	Pb* (pg)	Pb$_c$ (pg)	Th/U	U (ppm)	$^{206}Pb/^{204}Pb$	$^{207}Pb/^{206}Pb$	$^{206}Pb/^{238}U$	$\pm 2\sigma$	$^{207}Pb/^{235}U$	$\pm 2\sigma$	$^{206}Pb/^{238}U$ age (Ma)	$^{207}Pb/^{235}U$ Age (Ma)	$\pm 2\sigma$	$^{207}Pb/^{206}Pb$ age (Ma)	$\pm 2\sigma$	Disc. (%)	Correlation coefficient
KB-2 Medium-grained gabbro, Yeragumballi dyke, site 2																			
Bd-1	MAH5083	2 dbr, fl, larger eq. blades	0.0005	83.9	0.8	0.01	386	7082	0.15190	0.43743	0.00098	9.1612	0.0238	2339.1	2354.2	4.4	2367.4	1.9	1.4	0.9048
Bd-3	MAH5085	3 mbr, fl, long prismatic	0.0010	103.6	1.1	0.01	239	5897	0.15179	0.43637	0.00090	9.1329	0.0231	2334.4	2351.4	4.0	2366.2	1.8	1.6	0.9163
Bd-4	MAH5088n	3 pbr, fl, short prismatic	0.0002	105.2	1.3	0.01	120	5103	0.15179	0.44102	0.00094	9.2298	0.0237	2355.2	2361.1	4.2	2366.1	2.1	0.6	0.8818
Bd-5	MAH5093n2	2 mbr, fl blade and frag	0.0001	77.7	1.3	0.01	256	3757	0.15186	0.43683	0.00089	9.1467	0.0240	2336.4	2352.8	4.0	2367.0	2.3	1.5	0.8630

Notes: All analyzed fractions represent least magnetic, air-abraded single zircon grains, free of inclusions, cores or cracks, unless otherwise noted. Abbreviations: pbr—pale brown; mbr—medium brown; dbr—dark brown; eq—equant; euh—euhedral; fl—flat; frag—fragment. Pb* is total amount (in picograms) of radiogenic Pb. Pb$_c$ is total measured common Pb (in picograms) assuming the isotopic composition of laboratory blank: 206/204–18.221; 207/204–15.612; 208/204–39.360 (errors of 2%). Pb/U atomic ratios are corrected for spike, fractionation, blank, and, where necessary, initial common Pb; 206Pb/204Pb is corrected for spike and fractionation. Th/U is model value calculated from radiogenic 208Pb/206Pb ratio and 207Pb/206Pb age assuming concordance. Disc. (%)—percent discordance for the given 207Pb/206Pb age.

Table 3
Summary of paleomagnetic results for component A

SITE	Location LAT (°N); LONG (°E)	T (°)	W (m)	n/N/c	D (°)	I (°)	P_{lat} (°N) (− = °S)	P_{lon} (°E)	k	$\alpha 95$ (°)
2	12.01; 77.02	290	~25	**17/15**	**150.2**	**−84.0**	**22.2**	**70.7**	**150**	**3.1**
3*	11.98; 77.03	308	~40	11/7	40.9	−82.0			29	11.5
3**	11.98; 77.04			3/3	62.6	−71.8			27	26.6
3	11.98; 77.04			14/10	51.6	−79.2	−1.3	60.8	27	9.5
4	11.98; 77.03	290	~50	8/7	50.2	−70.5	−11.1	50.1	27	11.9
3 + 4	11.98; 77.03	300	~45	**22/17**	**50.8**	**−75.6**	**−5.6**	**56.2**	**26**	**7.1**
5	12.09; 77.39	285	~60	9/4	39.4	−78.5	−5.2	63.5	22	19.8
8	17.24; 80.13	250	~130	5/2/1	74.9	−86.0	15.0	72.2		
11	12.10; 76.70	295	20	6/2/3	115.8	−73.7	23.3	47.0	265	6.5
12	12.04; 78.52	290	15	**8/8**	**125.8**	**−71.3**	**29.6**	**47.0**	**55**	**7.6**
16*	12.58; 77.98	276	40	9/7	26.5	−80.6			73	7.1
16**	12.58; 77.98			3/3	67.7	−79.6			44	18.7
16	12.58; 77.98			**12/10**	**39.4**	**−80.9**	**−1.3**	**66.8**	**63**	**6.1**
17	12.63; 78.07	270	50	**5/5**	**186.4**	**−84.8**	**22.9**	**79.3**	**36**	**13.0**
18*	12.63; 78.07	255	15	4/4	76.6	−72.7			24	19.1
18**	12.63; 78.07			4/4	131.0	−70.9			42	14.4
18	13.49; 76.58			**8/8**	**105.4**	**−73.7**	**19.4**	**45.5**	**25**	**11.2**
19	13.51; 76.57	270	20	5/3	94.9	−77.5	14.3	51.9	294	7.2
20	14.31; 76.63	270	20	**8/5**	**72.8**	**−76.4**	**5.6**	**51.9**	**66**	**9.5**

Notes: Results in bold type satisfy acceptance criteria of $N \geq 4$ and $\alpha_{95} \leq 15°$. Sites 3 and 4, from the same dyke, are combined. *n/N*/c: number of collected samples/number giving remanence direction/number of other samples giving remagnetizatization circles. Other headings as in Table 1. * Dyke, ** Host rock. Mean directions and paleomagnetic pole for directions satisfying acceptance criteria are given in Table 5.

5.3. Paleomagnetism

A summary of paleomagnetic results shows that sites either have a steep upward magnetization A (Table 3) or one (B) with a northerly declination and low incli- nation (Table 4). One other component, found in sites 5 and 26 and designated C, lies in the SW quadrant (Table 4). The distribution of sites having these pale- omagnetic attributes is shown in Fig. 2. A summary of the paleomagnetic results is given in Fig. 7 with refer-

Table 4
Summary of paleomagnetic result for components B, A reversed, and C

SITE	Location LAT (°N); LONG (°E)	T (°)	W (m)	n/N	D (°)	I (°)	P_{lat} (°S)	P_{lon} (°E)	k	α_{95} (°)
Component B										
3 + 4	11.98; 77.03	300	~45	22/3	358.3	−2.5	−77.4	100.6	89	13.1
5	12.09; 77.39	285	~60	9/8	**355.4**	**−8.5**	**−73.0**	**93.3**	**35**	**9.5**
6	12.08; 77.27	285	~50	8/7	**353.3**	**−0.8**	**−75.9**	**105.8**	**58**	**8.0**
7	12.13; 77.56	300	~30	8/8	**001.1**	**−10.8**	**−72.4**	**73.9**	**88**	**6.0**
9	12.19; 77.62	290	~40	4/4	003.3	−14.1	−70.4	67.8	27	18.1
12	12.04; 78.52	290	15	8/1	005.2	14.8	−83.2	29.4	–	–
13	12.04; 78.51	305	20	10/7	**003.1**	**1.3**	**−78.2**	**63.2**	**137**	**5.2**
14	11.98; 78.45	280	30	10/8	**006.9**	**16.6**	**−82.4**	**15.1**	**142**	**4.7**
15	12.00; 78.47	310	30	9/7	**008.0**	**12.1**	**−80.2**	**24.4**	**137**	**5.2**
16	12.58; 77.98	275	~40	12/6	**353.1**	**3.2**	**−77.1**	**110.4**	**39**	**10.9**
Component A (reversed)										
10	11.89; 76.95	300	~30	6/5	**29.5**	**70.2**	**−19.4**	**59.2**	**196**	**5.5**
23	13.80; 76.91	270	~20	8/5	35.7	82.4	−25.7	86.5	15	20.8
Component C										
5	12.09; 77.39	285	~60	9/3	201.1	−40.6	−67.1	315.5	56	16.6
26	15.31; 76.49	280	~25	6/5	212.4	−43.7	−58.1	322.5	18	18.5

Notes: Headings are the same as in Table 3. Results in bold type satisfy the acceptance criteria of $N \geq 4$ and $\alpha_{95} \leq 15°$. Mean directions and paleomagnetic pole position for accepted component B data are given in Table 5.
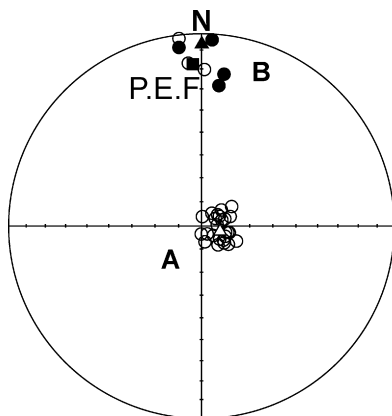
Fig. 7. Equal area stereoplot summarising the paleomagnetic data at the site (dyke) level, for component A and B. On this and subsequent plots open/closed symbols refer to upward/downward pointing vectors. The black square refers to the direction of the Present Earth's Field. Triangles represent the mean direction in each cluster.

ence to Table 5. Note in Fig. 7 that site directions for component A are extremely well clustered, but caution should be exercised in interpreting this low dispersion to secular variation, because the dykes have been assigned to the same swarm based in part on their paleomagnetic direction, thus reducing the dispersion of the data.

The characteristics of the A component is that it is generally carried by the highest coercivity and unblocking temperature grains, and is especially well-developed in southern dykes. At three sites (3, 16 and 18) it is also found in adjoining baked host rocks where the direction compares favourably with that from the dyke (Fig. 8, compare A with C and D; E with F, and G with H). Thermal demagnetization and susceptibility-temperature data show that the component is carried by magnetite (Fig. 8D). Only at one site (16) is there a host rock determination in unbaked charnockite (Fig. 8B); although the direction is clearly distinct from that of the dyke, it has a direction similar to that given by the Cretaceous Deccan plateau basalts. However, the component is not seen in any of the sampled dykes suggesting that heat or chemical activity from overlying Deccan flood

basalts has been minimal. An extensive study of the Archean host rocks in the region by Piper et al. (2003) has also failed to find any widespread re-heating by the Deccan volcanics, but more importantly the A component is only weakly represented in the magnetic signature of the Archean rocks; it does not form one of the contoured nodes that defines the interpreted components (see Piper et al., 2003, their Fig. 17), suggesting that the baked contact test is positive and that the A component is primary.

At site 10 (Table 4) interior samples gave a steep down component but samples collected closer to the margin yielded the A direction. The A direction may be primary if the growth of magnetite, responsible for the feldspar clouding in the interior was sufficiently slow that the critical blocking diameter was exceeded after a reversal of the field. Another example of a reversed A component is found at site 23 (Table 4) but only interior samples were available. The only other E-trending dyke with reversed A is that reported by Bhalla et al. (1980) from the Sargur area (Fig. 1). However, steep down directions may not necessarily correspond to a reversed A field because they have been found by Dawson and Hargraves (1994) in N-trending ~800 Ma alkaline dykes at location A in Fig. 1.

Component B, like A, is carried by magnetite (as determined from thermal demagnetization and susceptibility-temperature data), and when occurring as the only coherent component, has a high coercivity and unblocking temperature spectrum (Fig. 9A–D), but when accompanying component A, B has a lower coercivity and unblocking temperature spectrum (Fig. 9E and F). An important empirical observation is that B occurs alone or dominates in only those sites that display feldspars having the black clouding (i.e. sites 6, 13, 14, 15, 7 and 9). Since the sooty development appears to mask or form at the expense of the original brown-coloured clouding, the implication is that the B component is younger than A and is associated with the alteration. Some coarse-grained samples from dyke interiors show that B has an extremely high coercivity (Fig. 9A and C) and therefore could be residing in the small "sooty" inclusions. In these cases B could be

Table 5
Mean site directions and paleomagnetic poles for Components A and B

Component	Number of dykes	Mean D (°)	Mean I (°)	k	α_{95} (°)	P_{lat} (°N)	P_{lon} (°E)	A_{95} (°)
A								
Published	18	102.6	−78.5	95	3.6	16.5	55.8	6.3
This paper	7	94.9	−80.9	69	7.3	13.6	59.6	13.9
Combined	25	99.0	−79.4	83	3.2	15.7	56.9	5.6
B								
This paper	7	00.1	1.9	48	8.8	78.8	257.3	6.0

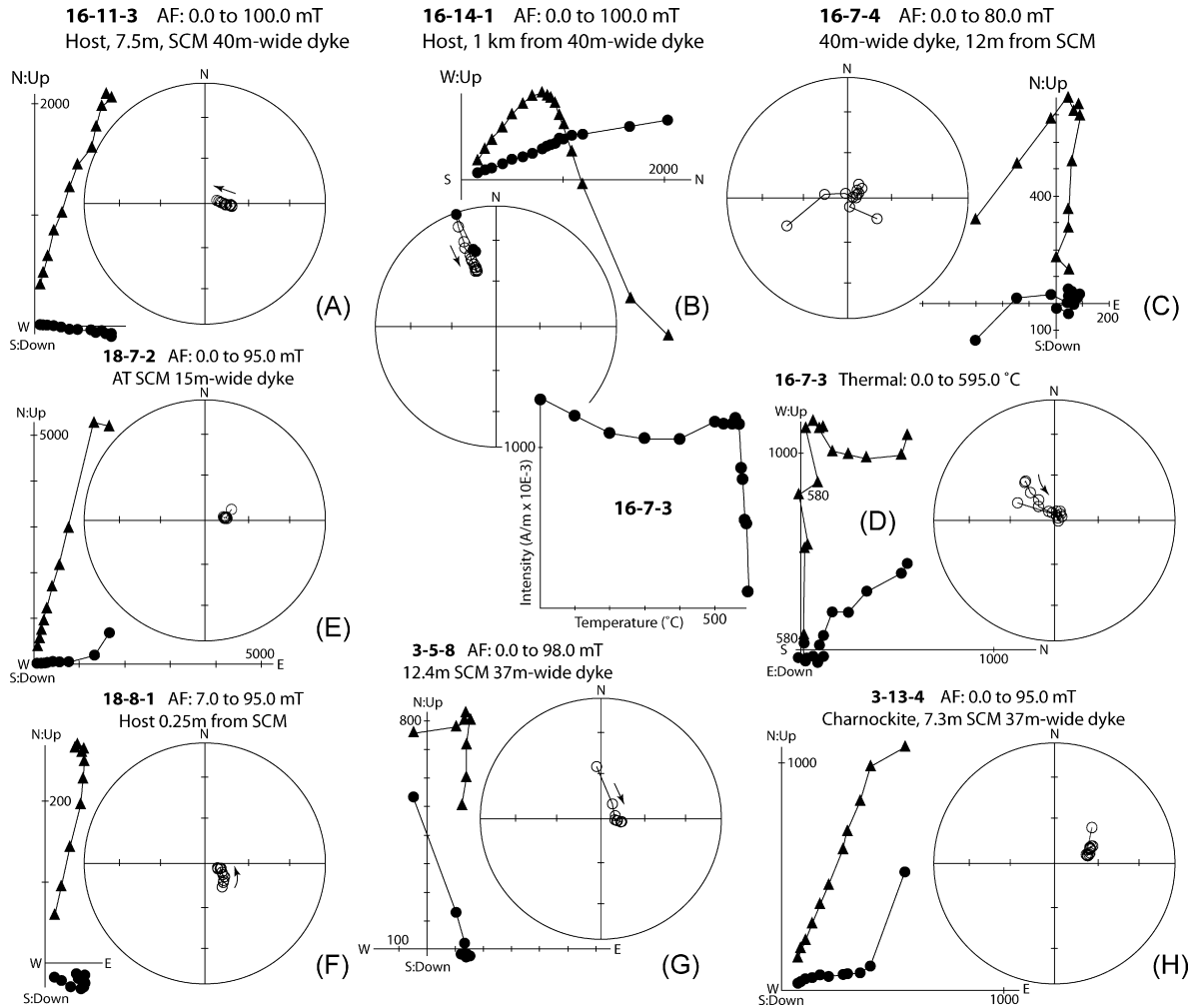*Note:* A_{95} is the half angle of the 95% confidence circle about the mean pole.

Fig. 8. Vector diagram and equal area stereonet pairs showing the behaviour of natural remanence to AF and thermal demagnetization for dyke and baked host rock specimens that carry the A component: site 16: diagrams A, C, D; site 18: diagrams E and F; site 3: diagrams G and H. A host rock specimen remote from baking is shown for site 16 in diagram B. Diagram D is a thermal decay plot demonstrating that magnetite is the remanence carrier at site 16. Vector diagrams show the projection, after each demagnetization step, of the end of the magnetization vector, onto two orthogonal planes, the horizontal one (black dots) and a vertical one, either N-S as in diagrams A, C, E, F, G and H, or E–W as in B and D (black triangles). Specimen captions indicate respectively, sample number, demagnetization treatment, and location; SCM/NCM is southern/northern dyke chilled margin. The intensity scale on the vector diagrams in this and subsequent figures is in $Am^{-1} \times 10^{-3}$.

produced through the growth of magnetite particles. At some sites that show only brown clouding, such as sites 3, 4, and 16, B is sometimes present but confined to chilled margins where NRM intensities are lower than in the interior, suggesting that, locally, B can also be produced chemically by fluids moving along the relatively fractured region of the dyke contact.

Site 5 has a conspicuous sooty development of its feldspars, but shows an interesting interplay upon AF and subsequent thermal demagnetization between three components A, B and C (Fig. 10). Both the B and C components are two of four major components identified in the Archean host rocks by Piper et al. (2003). During

AF demagnetization the B component is first destroyed whereupon the magnetization direction moves towards C. It may move along a great circle path (Fig. 10A), suggesting that only the two components are present but can also show a kink in the path that belies the presence of component A (Fig. 10B and C), which is revealed because it has a coercivity spectrum that lies with only partial overlap between the spectra of B and C, and remains after most of the C magnetization has been destroyed, close to the magnetite unblocking temperature, by subsequent thermal demagnetization.

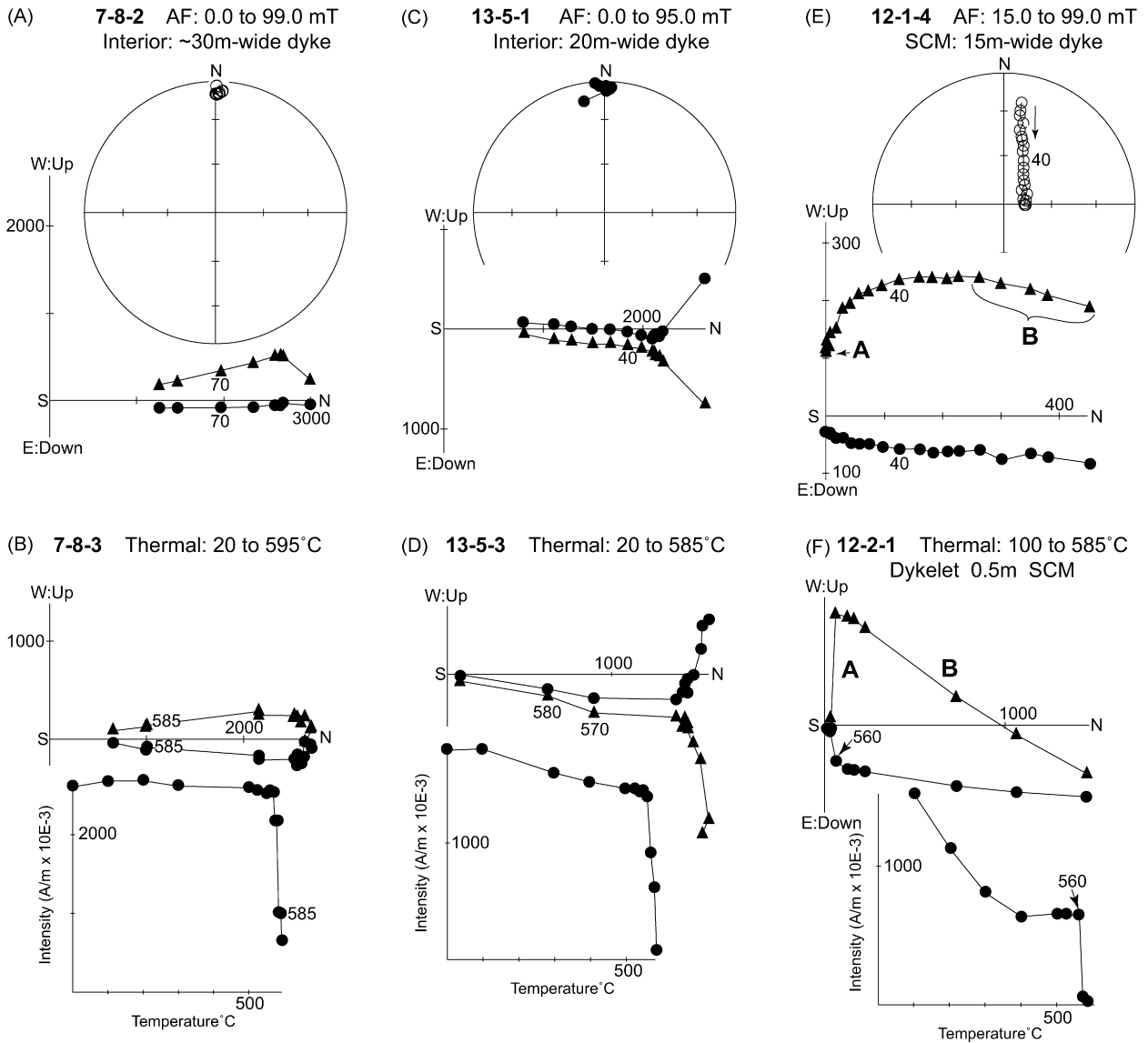The A component is most conspicuous in more southerly sites where dyke trends change from WNW

Fig. 9. Vector diagrams, equal area stereonets and thermal intensity decay plots illustrating the behaviour under AF and thermal demagnetization of component B for samples from three dykes. The component is carried by magnetite in all samples and occurs either alone (A–D) or with component A (E, F). Note in E and F that magnetization B has a lower coercivity spectrum and unblocking temperature compared to A. Symbols and explanation of diagrams as in Fig. 7.

to more E–W towards the north (Fig. 2). In the extreme northern part of the study area, north of site 20, where dykes with NE trends occur, the presence of component A is less secure. The northern sites are all from surface outcrops where chilled margins are either poorly preserved or lightning-struck and where the dykes show a higher level of hydrous alteration compared to those in the south. Site 23 gave a direction antipodal to A, site 26 gave the C component direction (Table 4), and the rest (sites 21, 24, 25 and 8) yielded scattered paleomagnetic data. At site 8 (north of the Cuddapah basin,

see Fig. 1 inset) where only the interior of a 130 m-wide dyke is exposed in shallow quarries along a ridge, all samples are completely remagnetized by lightning except for one which shows movement towards A at the highest coercivities. The dyke shows local clouding of the feldspars which may account for the survival of an A-type remanence in the coarse grained interior.

The paleomagnetic study has therefore identified a dyke swarm about 300 km wide which shows a change in trend from 300° in the south to ~270° in the north, defining a fan angle of about 30°. Farther north, dykes

(A)

5-2-4 AF: 5 to 58 mT
+ Thermal: 525 to 583°C

(B)

5-5-3 AF: 5 to 59 mT
+ Thermal: 538°C to 590°C

(C)

5-8-1 AF: 3 to 58 mT
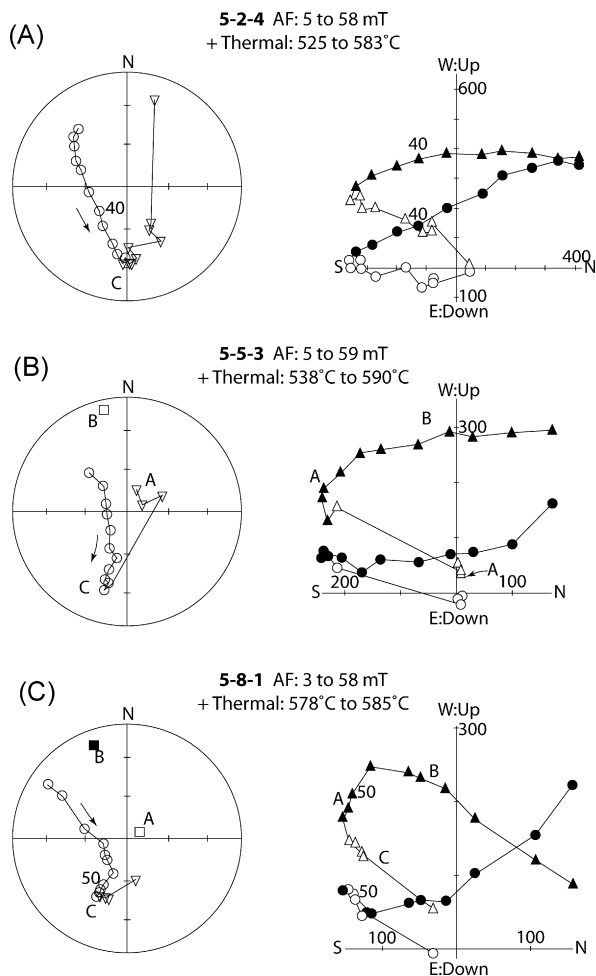+ Thermal: 578°C to 585°C

Fig. 10. Examples of thermal demagnetization after AF, of three interior samples from the dyke at site 5. In vector diagrams the solid/open triangles and dots are from AF/ thermal demagnetization. In diagram A an approximate linear decay to the origin signifies that only component C remains. In diagrams B and C all three components A, B and C can be identified. Solid/open squares in stereoplots indicate directions of components derived from principal component analysis (Kirschvink, 1980). See Fig. 7 for explanation of diagrams. Note in diagram B that it is possible that component A is being carried by hematite. However, the result is anomalous because thermal demagnetization and susceptibility-temperature runs for all other samples show that A is carried by magnetite.

with a more SW trend occur in the vicinity of Hyderabad and still farther north as the Karimnagar swarm (Rao et al., 1990). The age of these dykes is presently unknown, but paleomagnetically they yield directions with NE declination and shallow (∼20°) negative inclinations, similar to those obtained from charnockitic host rocks (Bhimasankaram, 1964). These directions are completely different from component A although some streaking towards higher negative inclinations is seen (Fig. 8 of Rao et al., 1990). The large α_{95} site values that

average more than 25° for Karimnagar dykes, the occurrence of the shallow inclination direction in presumably unbaked charnockites, and the presence of N-trending dykes in the Karimnagar area which also have the same direction (Rao et al., op cit), all suggest that the Karimnagar dykes are not recording a primary magnetization and may for example have been magnetically reset by the 2.1 Ga event recorded by Pandey et al. (1997) in the same region. Alternatively, they represent a dyke set that is older than 2367 Ma because a shallow negative magnetization with NE declination was recorded by Kumar and Bhalla (1983) from a dyke that on cross-cutting relations
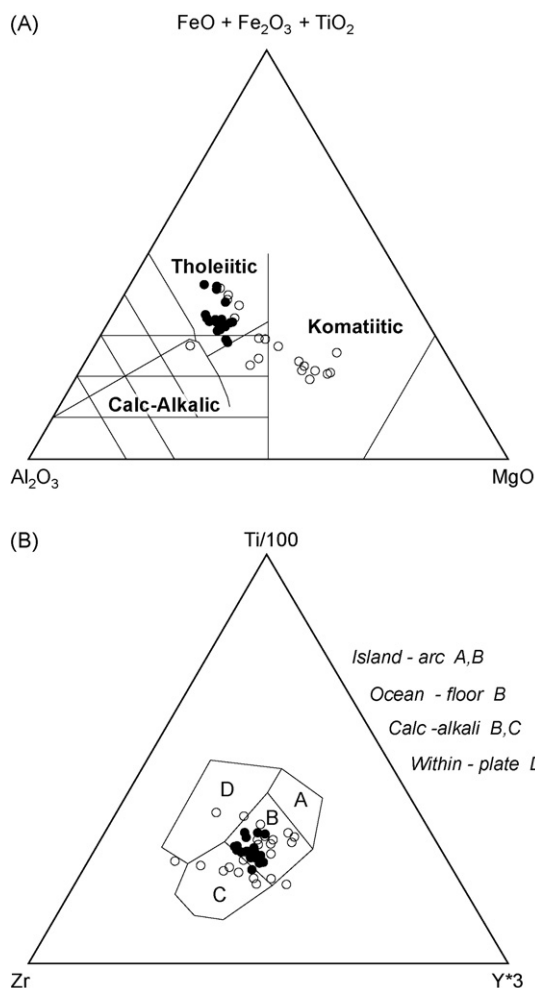

Fig. 11. Geochemical data from dyke chilled margins for the Indian (Tables A1 and A2 in Appendix A) and Widgiemooltha dykes in Australia (Hallberg, 1987). Note in the Jensen (1976) plot (Diagram A) the Indian data (black dots) are closely grouped, but the Widgiemooltha data (open dots) include more MgO-rich dykes. In the Pearce and Cann (1973) plot (Diagram B) the Indian data are closely grouped and are basically the same as the Widgiemooltha data. For both data sets, where more than one chilled margin sample has been analysed, only one analysis for that dyke is used.

was older than one carrying the A component. Further paleomagnetic investigations that concentrate on chilled margins and those dykes towards the northeastern end of the swarm where cloudy feldspars are observed (see Halls and Zhang, 1995) may resolve the issue.

5.4. Geochemistry

Major and minor element geochemical results from fresh chilled margins show (Fig. 11) that the dykes are iron-rich tholeiites, with MgO typically about 5 wt.%, TiO_2 about 1.5 wt.% and Fe_2O_3 at about 14–17 wt.% (Table A1). They show that all the dykes, whether from black-clouded feldspar dykes like sites 6 and 14, or from brown-clouded ones like 3, 10 and 19, have extremely similar compositions consistent with their being from the same swarm. However, Table A2 shows that dyke 25 with a trend of 265° has distinctly higher Ba and lower Y/Zr values, suggesting it may not share the same petrogenesis as the other dykes. Preliminary U–Pb results from two fractions of baddeleyite from this dyke suggest a primary crystallization age of approximately 1894 Ma, indicating that dyke 25 could be a feeder to the Cuddapah sills, and therefore is distinct from the older 2367 Ma diabase swarm that is the focus of this study.

6. Discussion

The direction of the B component (Fig. 7) is close to that of the Present Earth's field ($D = 358°$, $I = +10°$) so it could be ascribed to relatively recent tropical weathering. However, in many southern sites (e.g. 3, 5 and 16) that show B in addition to A, samples were taken from deep quarries, where recent weathering extends 2–3 m below the surface. Also in these sites and others (6, 7, 9, 13, 14 and 15) where only B is found, the dykes do not show any evidence of hydrous alteration; the feldspars and pyroxene are as fresh as in other southern sites. The only difference in thin section appears to be in the nature of the feldspar inclusions whereby those samples showing component A have feldspars that show the brown tea-colour clouding, and those that show B have cloudy areas that are completely or partially converted to the sooty appearance. Therefore some metamorphic event under dry crustal conditions may be responsible. Whatever the nature of the event it occurs over a distance of about 300 km being recorded in two areas of dykes (sites 13–15 and 5–9) and also from dykes in between which also carry the B remanence (see Fig. 2 and Table 2 of Radhakrishna and Joseph, 1996). A curious property of the alteration is that it occurs locally often within a few kilometres of dykes with brown feldspar cloud-

ing that display only the A remanence. The area of B remanence closely coincides with the major Pan African shear zone (Drury and Holt, 1980; Meissner et al., 2002), which lies less than 30 km south of our most southerly sites in the Henur area, but appears to pass through the region where sites 13–15 are located (Figs. 2 and 5). The lack of secondary hydrous minerals in the dykes carrying sooty feldspars suggests that the conversion from brown to sooty clouding has involved an alternative fluid such as CO_2. A B-like component, found in Archean host rocks, is more common in the SE part of Fig. 1 (Piper et al., 2003) where carbonatite igneous activity at ~800 Ma is most common. About 5 km east of Salem, SW of the Harur sites (Fig. 1) plagioclase in charnockites has developed clouding close to carbonatite veins (R. Srinivasan, unpublished data) and fenitization of the host rocks in the vicinity of the carbonatites has been reported (Borodin et al., 1971). These observations suggest that CO_2-charged magmatic fluids associated with carbonatite emplacement are capable of causing the sooty clouding. Charnockite formation during the ~550 Ma Pan- African orogenic cycle has been reported from south of the shear zone (Santosh et al., 2003) so that CO_2 flushing associated with this event (e.g. Piper et al., 2003) may also be responsible for the sooty clouding and hence the B component. In terms of their petrography, geochemistry, and the occasional survival of the A component, as in site 5, dykes exhibiting sooty feldspar clouding are similar to the dykes with brown clouding. Their trend is also similar except in the extreme southeast where dykes at sites 13–15 have a more NW trend. However, these dykes show more signs of shearing, appear to lie within the shear zone, and therefore may have been rotated. One important point is that if the B component is caused by ~550 Ma charnockite formation and/or by 800 Ma carbonatite activity, its direction is very different from the steep direction recorded in the ~800 Ma Harohalli alkaline dykes by Dawson and Hargraves (1994), although the highly altered nature of these dykes renders the primary nature of their pole uncertain. The B pole lies close to the Indian apparent polar wander path, about 30° from that of the 760 Ma Malani rhyolite in NW India (Torsvik et al., 2001) on the younger side of the Indian apparent polar wander path, so we surmise that the Neoproterozoic was characterised by shallow rather than by steep inclinations in southern India.

Important conclusions from our observations are that a primary component (A) resides in dykes with brown feldspar clouding and that a secondary (B) magnetization is preserved in those dyke with black feldspar clouding. The precise mechanism by which the sooty clouding has formed is unknown, but we may speculate that CO_2,
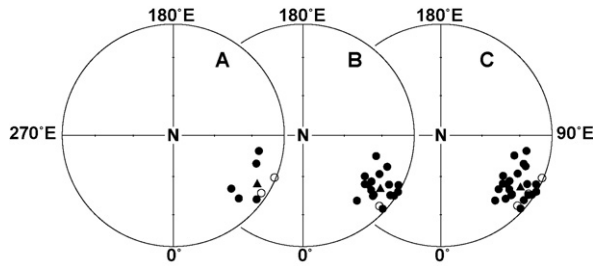
Fig. 12. Equal area stereoplots showing site virtual geomagnetic poles corresponding to the A component. (A) All sites from this work that pass the reliability criteria (N, number of samples ≥4, $\alpha_{95} \leq 15°$) according to Table 2; (B) all previously published results that fulfill the same reliability criteria according to Table 1; (C) data sets combined. Triangles are the mean pole positions, the statistics for which are given in Table 5. Solid/open dots correspond to northern/southern latitude pole positions.

produced during the ∼800 Ma carbonatite event and/or by later charnockite formation associated with the Pan-African orogen, combined with Fe in the feldspar to produce magnetite and carbon. We would envisage that this process would be pervasive at deep crustal levels, but could also occur at shallower depths where CO_2 could move along dyke chilled margins (such as at site 3) and other potential zones of fracture. Scanning electron microscopy shows that micron to sub-micron grains include magnetite, and that many smaller ones, as opposed to few larger ones, seem to respectively characterize the sooty and brown clouding types, but further work is required to examine the feldspars for carbon. Regardless of the exact mechanism by which the sooty clouding is produced, our empirical observations suggest that petrographically fresh diabase dykes exhibiting plagioclase feldspars with a black, rather than brown clouding, have been remagnetized.

Component C is found as the characteristic component in one dyke (No. 26, Table 2) and therefore may signify a different magmatic episode. The same direction occurs along with A and B at site 5 and has been reported from NNW trending dykes in northern Kerala by Radhakrishna et al. (1986) and also as a significant component in the Archean host rocks (Piper et al., 2003, their Fig. 17).

The mean pole position for the A component incorporating the present data and with the site acceptance criteria of $N \geq 4$ and $\alpha_{95} \leq 15°$ gives a pole position of $P_{lat} = 13.6°N$, $P_{long} = 59.6°E$, $N = 7$ and $A_{95} = 13.9°$ or its antipode (Fig. 12A). Our pole results agree at the 95% confidence level with the mean pole position calculated from all published data satisfying the same acceptance criteria (Fig. 12B, Table 5). The combined pole position using all the data is: $P_{lat} = 15.7°N$, $P_{long} = 56.9°E$,

$N = 25$ and $A_{95} = 5.6°$ (Fig. 12C). One important observation, seen in both independent data sets (Fig. 12A and B) is a bimodal separation of basically equatorial paleopoles versus others of higher paleolatitude. Explanations for the bimodal behaviour are either that two dyke populations of different age are represented, or that the lower paleolatitudes are the result of contamination of component A by B or B-like components. All samples contributing directional estimates to Fig. 12A were examined for the presence of component B. It was found that 44 samples yielding A remanence declinations in the SE quadrant and thus the higher latitude paleopoles, whether from dyke or host rock, were 100% free of component B. However, of 31 samples with A declinations in the NE quadrant and thus yielding the lower latitude paleopoles, two thirds contained the B component. On average the former group more frequently gave stable end-points whereas the latter one gave linear segments that did not pass through the origin or were less well-determined while still passing the acceptability criteria for linearity. The conclusion is that below about 5% of NRM intensity where many A segments were defined, B-like components may still contaminate the data. However, the lack of streaking and the formation of a cluster of poles that become less Fisherian after removal of the low latitude poles, suggests that the combined mean of all the data is probably the best estimate of the pole position, as given in Table 5.

A search of the IAGA Global Paleomagnetic data base (http://dragon.ngu.no) and the compilation by Ernst and Buchan (2001) does not reveal any other dykes with well-determined primary paleomagnetic poles and an age similar to 2367 Ma. The closest age is that for the Widgiemooltha dykes in western Australia (2410–2418 Ma, Doehler and Heaman, 1998; Nemchin and Pidgeon, 1998), which also cut orthogonally across the structural grain of granite-greenstone belts in the Archean Yilgarn block. A continental reconstruction (Fig. 13) shows that India and Australia are both at high paleolatitudes, and that the dyke trends (and greenstone belts) can be made similar at the closest approach of the two cratons when they are only about 2000 km apart. Since paleolongitude is not constrained by the paleomagnetic data, either continent is free to move around its paleolatitude. In Fig. 13 two positions of India are shown to illustrate that the two sets of dykes may represent segments of a giant radiating swarm, centred approximately at the pole, that are either close together or far apart. The 50 My age difference between the Indian and Widgiemooltha dykes does not necessarily mitigate against them being the product of a single plume. In the Lake Superior Region a large radiating swarm, with
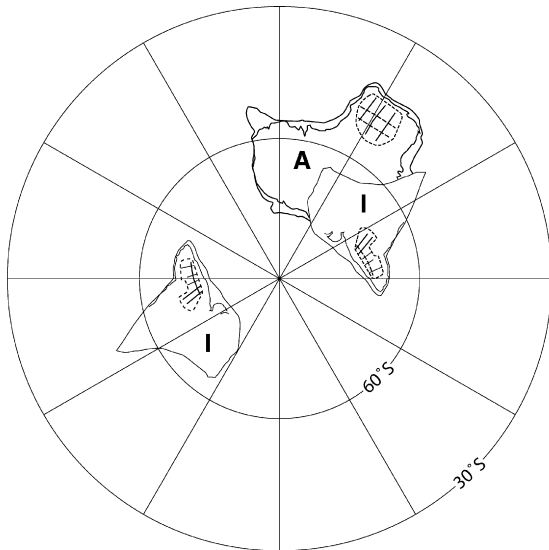
Fig. 13. South polar projection showing two positions of the Dharwar craton of India (I) with respect to the Yilgarn Craton of Australia (A), based on paleomagnetic results of this work for the 2367 Ma Dharwar dykes and those of Evans (1968) for the 2415 Ma Widgiemooltha dyke suite. Cratonic areas are shown with Archean structural trends drawn as dashed lines and dykes as solid lines. Figure produced using the GMAP software of Trond Torsvik, Norwegian Geological Survey, Trondheim.

a fan angle of possibly up to 140° and a plume centre immediately south of Lake Superior, has an age range from 2125 to 2067 Ma (Halls et al., 2005; Schmitz et al., 2006). The nearby Matachewan swarm has an age range from at least 2446 to 2473 Ma (Heaman, 1997) and may also represent a period of magmatic activity about 50 My long if gabbro–anorthosite bodies of the 2490–2475 Ma East Bull Lake intrusive suite (James et al., 2002), found in the focal region of the swarm, are related. Both radiating swarms suggest a long-lived and episodic plume that was virtually stationary during each magmatic "event". It is therefore speculated that the Dharwar and Widgiemooltha dykes also represent part of a long-lived plume from which the dykes radiate. The Widgiemooltha swarm has, like the Indian dykes, an overall tholeiitic composition (Hallberg, 1987) but contains more olivine-bearing, more MgO-rich, dykes towards the centre of the Yilgarn block (Fig. 11A). However a Ti–Zr–Y plot (Pearce and Cann, 1973) cannot distinguish between the two dyke sets (Fig. 11B). Detailed incompatible trace element investigations that may be able to demonstrate a genetic connection have yet to be carried out on either swarm.

7. Conclusions

U–Pb geochronological and paleomagnetic data suggest that a major radiating dyke swarm, at least 300 km wide and with an age of 2367 ± 1 Ma, crosses the Dharwar craton of India. The associated paleomagnetic pole, derived from a primary remanence, suggests that India was at high latitudes at this time. Despite the uncertainty in paleolongitude, a position for the Dharwar craton can be found that is only about 2000 km away from the Yilgarn craton in Australia as given by 2415 Ma Widgeimooltha dykes, and is such that the dyke trends are similar. Given the observation that some Paleoproterozoic radiating swarms have durations of the order of 50 My, it is possible that the Widgiemooltha and Dharwar dyke suites have issued from a common plume centre.

A comparison of the paleomagnetic response from Dharwar dykes differing only in the character of their feldspar clouding, suggests that black feldspar clouding is a carrier of secondary magnetization, in this case probably associated with Neoproterozoic carbonatite activity at 800 Ma and/or with Pan-African charnockite formation at ~550 Ma, whereas diabase with brown clouding yields a magnetization that is more likely to be primary or temporally close to primary. This is an important observation given that the characteristic component in many dykes is defined only at the highest coercivities, where magnetite inclusions in feldspar are likely to form a significant fraction of the magnetic carriers.

Table A1
Major element analyses in weight percent.

Sample	SiO_2	Al_2O_3	CaO	MgO	Na_2O	K_2O	Fe_2O_3	MnO	TiO_2	P_2O_5
3–8	52.8	13.1	9.6	5.31	2.42	0.78	14.1	0.19	1.23	0.18
3–1B	53.5	13.2	9.35	4.80	2.46	0.84	13.9	0.19	1.21	0.18
3–11	52.8	13.6	9.44	4.76	2.53	0.84	14.5	0.19	1.29	0.19
4–1	52.3	13.0	9.33	5.12	2.43	0.77	14.3	0.19	1.24	0.18
4–2	52.7	13.3	8.83	4.47	2.51	0.84	14.5	0.18	1.35	0.22
6–4	53.0	13.6	9.96	5.68	2.40	0.73	13.6	0.18	1.10	0.16
8–3	48.3	12.8	9.69	5.59	2.35	0.90	17.2	0.23	1.94	0.29
10–6	49.0	12.2	8.89	4.47	2.54	1.00	17.2	0.22	2.38	0.41
10–7	48.4	12.1	8.70	4.38	2.49	1.16	17.4	0.23	2.41	0.41
14–1	52.0	13.3	9.74	5.78	2.34	0.71	13.7	0.18	1.10	0.16
16–9	51.7	13.5	9.88	5.67	2.38	0.72	14.6	0.20	1.16	0.17
18–2	51.1	13.6	10.2	5.89	2.26	0.49	14.3	0.20	1.05	0.14
18–7	51.0	13.3	10.0	6.10	2.23	0.62	14.5	0.20	1.02	0.14
19–4A	52.1	13.8	10.6	6.69	2.21	0.61	12.8	0.18	0.90	0.12
19–5	52.2	13.8	10.5	6.59	2.16	0.55	13.0	0.18	0.92	0.13
23–2	50.1	13.1	10.3	6.52	2.26	0.33	15.2	0.21	1.33	0.19
24–1	49.3	13.6	9.96	5.83	2.22	0.47	15.5	0.20	1.21	0.15
25–1	52.0	12.0	8.05	3.53	2.42	1.42	16.8	0.20	2.04	0.27
25–2	52.2	12.1	7.93	3.50	2.37	1.54	16.8	0.19	2.05	0.27
25–9	52.3	12.1	7.91	3.47	2.50	1.47	16.9	0.20	2.08	0.27

Notes: Whole rock samples were analyzed, following crushing and pulverising in an agate mortar, at SGS Canada Ltd using X-ray fluorescence techniques on fused disks for major and minor elements and on pressed pellets for trace elements. Sample number notation: site followed by sample number. Samples are within 15 cm of chilled margins, except 8–3 which is from the interior of a 120 m wide dyke.

Appendix A

See Tables A1 and A2.

Table A2
Minor element analyses in parts per million

Sample	Rb	Sr	Y	Zr	Nb	Ba	Y/Zr
3–8	33	137	31	112	5	260	0.277
3–1B	33	136	27	111	5	280	0.243
3–11	33	139	30	113	5	260	0.265
4–1	33	133	31	108	5	270	0.287
4–2	32	141	37	121	7	290	0.306
6–4	30	145	28	102	5	260	0.275
8–3	33	163	37	145	11	290	0.255
10–6	37	144	50	155	9	320	0.323
10–7	43	141	48	162	10	340	0.296
14–1	30	138	29	100	6	280	0.290
16–9	29	136	28	102	5	260	0.275
18–2	22	129	28	91	5	200	0.308
18–7	IS	IS	IS	IS	IS	IS	IS
19–4A	29	129	26	85	3	190	0.306
19–5	29	136	27	85	5	190	0.318
23–2	11	149	24	96	5	120	0.250
24–1	21	122	28	99	7	120	0.283
25–1	39	183	41	181	10	550	0.227
25–2	44	184	43	186	10	590	0.231
25–9	43	187	42	182	8	550	0.231

Note: IS, insufficient sample.

References

Anand, M., Gibson, S.A., Subbarao, K.V., Kelley, S.P., Dickin, A.P., 2003. Early Proterozoic melt generation processes beneath the intracratonic Cuddapah basin, southern India. J. Petrol. 44, 2139–2171.

Anjannappa, K., 1975. Paleomagnetism and age of the dolerite dykes of the Tirupati area, Chittoor District, Andhra Pradesh. Recent Res. Geol. 2, 161–169.

Bhalla, M.S., Hansraj, A., Prasada Rao, N.T.V., 1980. Paleomagnetic studies of Bangarpet and Sargur dykes of Precambrian age from Karnataka, India. Geoviews 8, 181–189.

Bhaskar Rao, Y.J., Pantulu, G.V.C., Reddy, V.D., Gopalan, K., 1995. Time of early sedimentation and volcanism in the Proterozoic Cuddapah Basin, South India: evidence from the Rb–Sr age of the Pulivendla mafic sill. J. Geol. Soc. India 33, 329–338.

Bhimasankaram, V.L.S., 1964. A preliminary investigation on the paleomagnetic directions of the charnockites of Andhra Pradesh. Curr. Sci. 33, 465–466.

Borodin, L.S., Gopal, V., Moralev, V.M., Subramanian, V., 1971. Precambrian carbonatites of Tamil Nadu, south India. J. Geol. Soc. India 12, 101–112.

Chadwick, B., Vasudev, V.N., Hegde, G.V., 2000. The Dharwar craton, southern India, interpreted as the result of late Archean oblique convergence. Precambrian Res. 99, 91–111.

Dawson, E.M., Hargraves, R.B., 1994. Paleomagnetism of Precambrian swarms in the Harohalli area, south of Bangalore, India. Precambrian Res. 69, 157–167.

Doehler, J.S., Heaman, L.M., 1998. 2.41 Ga U–Pb baddeleyite ages for two gabbroic dykes from the Widgiemooltha swarm, west-

ern Australia: a Yilgarn Lewisian connection? Geol. Soc. Am. 30, A291–A292 (Abstracts with programs).

Drury, S.A., Holt, R.W., 1980. The tectonic framework of the South Indian craton: a reconnaissance involving LANDSAT imagery. Tectonophysics 65, T1–T15.

Ernst, R.E., Buchan, K.L., 2001. Large magmatic events trough time and links to mantle plume heads. In: Ernst, R.E., Buchan, K.L. (Eds.) Mantle Plumes: Their Identification Through Time, GSA Special Paper 352, pp. 483–575.

Evans, M.E., 1968. Magnetization of dikes: a study of the paleomagnetism of the Widgiemooltha dike suite, Western Australia. J. Geophys. Res. 73, 32361–33270.

French, J.E., Heaman, L.M., Chacko, T., Rivard, B., 2004. Global mafic magmatism and continental break-up at 2.2 Ga: evidence from the Dharwar Craton, India. Geol. Soc. Am. 36 (5), 340 (Abstracts with programs).

Friend, C.R.L., Nutman, A.P., 1991. SHRIMP U–Pb geochronology of the Closepet granite and Peninsula gneisses, Karnataka, South India. J. Geol. Soc. India 32, 357–368.

Gokhale, N.W., Waghamare, B.P., 1989. K–Ar ages on three basic intersecting dykes from Gadag schist belt, Karnataka. J. Geol. Soc. India 34, 663–664.

Hallberg, J.A., 1987. Postcratonization mafic and ultramafic dykes of the Yilgarn Block. Austr. J. Earth Sci. 34, 135–149.

Halls, H.C., 1978. The structural relationship between Archean granite-greenstone terrains and late Archean mafic dykes. Can. J. Earth Sci. 15, 1665–1668.

Halls, H.C., 1982. The importance and potential of mafic dyke swarms in studies of geodynamic processes. Geosci. Canada 9, 145–154.

Halls, H.C., 1991. The Matachewan dyke swarm, Canada: an early Proterozoic magnetic field reversal. Earth Planet. Sci. Lett. 105, 279–292.

Halls, H.C., Bates, M.P., 1990. The evolution of the 2.45 Ga Matachewan swarm, Canada. In: Parker, A.J., Rickwood, P.C., Tucker, D.H. (Eds.), Mafic Dykes and Emplacement Mechanisms. Balkema, Rotterdam, pp. 237–250.

Halls, H.C., Zhang, Z., 2003. Crustal uplift in the southern Superior Province, Canada, revealed by paleomagnetism. Tectonophysics 362, 123–136.

Halls, H.C., Zhang, B., 1995. Tectonic implications of clouded feldspar in Proterozoic mafic dyke swarms. Geol. Soc. India Memoir 33, 65–80.

Halls, H.C., Stott, G.M., Davis, D.W., 2005. Paleomagnetism, geochronology and geochemistry of several Proterozoic dike swarms in northwestern Ontario. Ontario Geological Survey Open File Report 6171, 59pp.

Hamilton, M.A., Davis, D.W., Buchan, K.L., Halls, H.C., 2002. Precise U–Pb dating of reversely magnetized Marathon diabase dykes and implications for emplacement of giant dyke swarms along the southern margin of the Superior Province, Ontario. Report 15, Current Research 2002-F6, Radiogenic age and Isotopic Studies, Geological Survey of Canada, pp. 1–8.

Hargraves, H.B., Bhalla, M.S., 1983. Precambrian paleomagnetism in India through 1982: a review. In: Naqvi, S.M., Rogers, J.J.W. (Eds.), Precambrian of South India, Geol. Soc. India Memoir 4, pp. 491–524.

Hasnain, J., Qureshy, M.N., 1971. Paleomagnetism and geochemistry of some dykes in Mysore State, India. J. Geophys. Res. 76, 4786–4795.

Heaman, L.M., 1997. Global mafic magmatism at 2.45 Ga: Remnants of an ancient large igneous province? Geology 25, 299–302.

Ikramuddin, M., Stueber, A.M., 1976. Rb-Sr ages of Precambrian dolerite and alkaline dykes, southeast Mysore State, India. Lithos 9, 235–241.

Jaffey, A.H., Flynn, K.F., Glendenin, L.E., Bentley, W.C., Essling, A.M., 1971. Precision measurement of half-lives and specific activities of 235 U and 238 U. Phys. Rev. C4, 1889–1906.

James, R.S., Easton, R.M., Peck, D.C., Hrominchuk, J.L., 2002. The East Bull Lake intrusive suite: remnants of a ~2.48 Ga large igneous and metallogenic province in the Sudbury area of the Canadian Shield. Econ. Geol. 97, 1577–1606.

Jensen, L.S., 1976. A New Cation Plot for Classifying Subalkalic Volcanic Rocks, vol. 66. Ontario Division of Mines, MP, pp. 1–22.

Kirschvink, J.L., 1980. The least squares line and plane and the analysis of paleomagnetic data. Geophys. J. R. Astron. Soc. 62, 699–718.

Kumar, A., Bhalla, M.S., 1983. Paleomagnetics and igneous activity of the area adjoining the south-western margin of the Cuddapah basin, India. Geophys. J. R. Astron. Soc. 73, 27–37.

Kumar, A., Nirmal Charan, S., Gopalan, K., Macdougall, J.D., 1998. A long-lived enriched mantle source for two carbonatite complexes from Tamil Nadu, southern India. Geochim. Cosmochim. Acta 62, 515–523.

Ludwig, K.R., 2003. Isoplot 3.00, a geochronological toolkit for Excel. Berkeley Geochronology Center Special Publication No. 4.

Meissner, B., Deters, P., Srikantappa, C., Kohler, H., 2002. Geochronological evolution of the Moyar, Bhavani and Palghat shear zones of southern India: implications for East Gondwana correlations. Precambrian Res. 114, 149–175.

Moyen, J.-F., Martin, H., Jayananda, M., Mahabaleswar, B., Auvray, B., 2003. From the roots to the roof of a granite: the Closepet granite, south India. J. Geol. Soc. India 62-6, 753–768.

Murty, Y.G.K., Babu Rao, V., Guptasarma, D., Rao, J.M., Rao, M.N., Bhattacharji, S., 1987. Tectonic, petrochemical and geophysical studies of mafic dyke swarms around the Proterozoic Cuddapah Basin, south India. In: Halls, H.C., Fahrig, W. (Eds.), Mafic Dyke Swarms, Geol. Assoc. Canada Special Paper, vol. 34, pp. 303–316.

Naqvi, S.M., Rogers, J.J.W., 1987. Precambrian Geology of India, vol. 6. Oxford University Press, Oxford, pp. 105–123.

Nemchin, A.A., Pidgeon, R.T., 1998. Precise conventional and SHRIMP baddeleyite U–Pb age for the Binneringie dyke near Narrogin, Western Australia. Austr. J. Earth Sci. 45, 673–675.

Pandey, B.K., Gupta, J.N., Sarma, K.J., Sastry, C.A., 1997. Sm–Nd, Pb–Pb and Rb–Sr geochronology and petrogenesis of the mafic dyke swarm of Mahbubnagar, south India: implications for Paleoproterozoic crustal evolution of the eastern Dharwar craton. Precambrian Res. 84, 181–196.

Pearce, J.A., Cann, J.R., 1973. Tectonic setting of basic volcanic rocks determined using trace element analysis: Earth Planet. Sci. Lett. 19, 290–300.

Pichamuthu, C.S., 1951. Clouded feldspars in basic dykes of charnockitic areas. Curr. Sci. 18, 230–231.

Pichamuthu, C.S., 1953. Some observations on the structure and classification of the Dharwars of Mysore State. Curr. Sci. 20, 117–119.

Pichamuthu, C.S., 1959. The significance of clouded plagioclase in the basic dykes of Mysore State, India. J. Geol. Soc. India 1, 68–79.

Piper, J.D.A., Mallik, S.B., Bandyopadhyay, G., Mondal, S., Das, A.K., 2003. Paleomagnetic and rock magnetic study of a deeply exposed continental section in the Charnockite Belt of southern India: implications to crustal magnetization and Paleoproterozoic continental nucleii. Precambrian Res. 121, 185–219.

Poornachandra Rao, G.V.S., 2005. Orthogonal dykes around the Cuddapah basin—a paleomagnetic study. J. Indian Geophys. Union 9, 1–11.

Radhakrishna, T., Poornachandra Rao, G.V.S., Mitchell, J.G., Venkatesh, A.S., 1986. Proterozoic basic dyke activity in Kerala along the western continental margin of India. J. Geol. Soc. India 27, 245–253.

Radhakrishna, T., Joseph, M., 1996. Proterozoic paleomagnetism of the mafic dyke swarms in the high grade region of southern India. Precambrian Res. 76, 31–46.

Rao, J.M., Rao, G.V.S.P., Patil, S.K., 1990. Geochemical and paleomagnetic studies on the middle Proterozoic Karimnagar mafic dyke swarm. In: Parker, A.J., Rickwood, P.C., Tucker, D.H. (Eds.), Mafic Dykes and Emplacement Mechanisms, pp. 373–382.

Santosh, M., Tagawa, M., Taguchi, S., Yoshikura, J., 2003. The Nagerkoil granulite block, southern India: petrology, fluid inclusions and exhumation history. J. Asian Earth Sci. 22, 131–155.

Schleicher, H., Kramm, U., Pernicka, E., Schidowski, M., Schmidt, F., Subramanian, V., Todt, W., Viladkar, S.G., 1998. Enriched subcontinental mantle beneath southern India: evidence from Pb, Nd, Sr, and C–O isotopic studies on Tamil Nadu carbonatites. J. Petrol. 39, 1765–1785.

Schmitz, M.D., Bowring, S.A., Southwick, D.L., Boerboom, T.J., Wirth, K.R., 2006. High-precision U–Pb geochronology in the Minnesota River Valley subprovince and its bearing on the Neoarchean to Paleoproterozoic evolution of the southern Superior Province. Geol. Soc. Am. Bull. 118, 82–93.

Swami Nath, J., Ramakrishnan, M. (Eds.), 1981. Early Precambrian Supracrustals of southern Karnataka. Memoir 112, Geological Survey of India, 363 pp.

Torsvik, T.H., Carter, L.M., Ashwal, L.D., Bhushan, S.K., Pandit, M.K., Jamtveit, B., 2001. Rodinia refined or obscured: paleomagnetism of the Malani igneous suite (NW India). Precambrian Res. 108, 319–333.

Venkatesh, A.S., Poornachandra Rao, G.V.S., Prasada Rao, N.T.V., Bhalla, M.S., 1987. Paleomagnetic and geochemical studies on dolerite dykes from Tamil Nadu, India. Precambrian Res. 34, 291–310.

Zachariah, J.K., Hanson, G.N., Rajamani, V., 1995. Postcrystallization disturbance in the neodymium and lead isotope systems of metabasalts from the Ramagiri schist belt, southern India. Geochim. Cosmochim. Acta 59, 3189–3203.